

ADA022704

20

Technical Progress Report 75-2 Final
July 1, 1975 to December 31, 1975

SENSITIVITY FUNDAMENTALS

By: T. MILL, D. S. ROSS, N. A. KIRSHEN, C. M. TARVER,
R. SHAW, and M. COWPERTHWAIT

Prepared for:

OFFICE OF NAVAL RESEARCH
DEPARTMENT OF THE NAVY
ARLINGTON, VIRGINIA

Contract N00014-70-C-0190

D D C
RECEIVED
APR 6 1976
RECEIVED
A



STANFORD RESEARCH INSTITUTE
Menlo Park, California 94025 • U.S.A.

DISSEMINATION STATEMENT A
Approved for public release;
Distribution Unlimited



STANFORD RESEARCH INSTITUTE
Menlo Park, California 94025 · U S A

Technical Progress Report 75-2 Final
July 1, 1975 to December 1, 1975

January 1976

SENSITIVITY FUNDAMENTALS

By: T. MILL, D. S. ROSS, N. A. KIRSHEN, C. M. TARVER,
R. SHAW, and M. COWPERTHWAIT

Prepared for:

OFFICE OF NAVAL RESEARCH
DEPARTMENT OF THE NAVY
ARLINGTON, VIRGINIA

Contract N00014-70-C-0190
NR. 092-537

NR -
SRI Project-PYU-8525

Reproduction in whole or in part is permitted for any purpose of the United States Government.

Approved by:

MARION E. HILL, *Director*
Chemistry Laboratory

CHARLES J. COOK, *Executive Director*
Physical Sciences Division

PREFACE

This project is the responsibility of the Chemistry Laboratory in the Physical Sciences Division of Stanford Research Institute, and is under the overall supervision of M. E. Hill, Laboratory Director. Project organization and principal contributors to the technical work are:

Project Supervisor:	T. Mill
HVD Phenomena:	C. Tarver, R. Shaw, M. Cowperthwaite
Thermal Decomposition:	D. S. Ross and N. Kirshen

ACKNOWLEDGEMENT

We thank Dr. Ralph Roberts and Dr. Richard Miller of the Office of Naval Research for continued interest and support of this research program for so many years.

ACCESSION list	
NTIS	<input checked="" type="checkbox"/>
ACC	<input type="checkbox"/>
DDC	<input type="checkbox"/>
...	...
BY	...
...	...
...	...
...	...

[Handwritten signature]

SUMMARY

This final report for the ONR-supported program on sensitivity fundamentals at SRI summarizes the results of five years of research on the kinetic and detonation properties of several dinitroalkanes. Three manuscripts are included as part of this report and are summarized below.

Thermal decomposition of neat, liquid 1,1-DNP at 1 and 1000 atm and 135-155°C gives over 90% propionic acid with small amounts of acetic acid with conversions ranging from 29% in 1.5 hours at 135°C and 1000 atm to 10% in 21 hours at 155°C and 1 atm. 2,2-DNP, in contrast, decomposed slowly at 165°C to give only acetone, NO and NO₂. Pressure retarded the reaction slightly. At 190°C 2,2-DNP had a half-life of 15 hours and gave with increasing conversion increasing amounts of acetic acid, CO₂, CO, and N₂O. Reactions of isobutane and neopentane with NO₂-N₂O₄ indicate that HNO₃ is an intermediate oxidizer in these reaction mixtures.

The unimolecular decomposition of four dinitropropanes has been studied in the gas phase using a low-pressure pyrolysis technique. 1,2-Dinitropropane was found to undergo cyclic elimination of HONO, giving 1- and 2-nitropropene. The rate constant for the process is $\log k (\text{sec}^{-1}) = 11.3 - 40/\Theta$. Three gem-dinitroalkanes, 1,1- and 2,2-dinitropropane and 1-fluoro-1,1-dinitropropane undergo C-N scission rather than HONO elimination, with essentially the same rate constant, $\log k (\text{sec}^{-1}) = 17.0 - (47 \pm 1)/\Theta$. Major decomposition products in these cases were propionaldehyde and acetone in the case of the 1,1- and 2,2-dinitropropanes, and propionyl fluoride in the case of 1-fluoro-1,1-dinitropropane.

The detonation failure diameters of four liquid nitroalkanes (nitromethane, 1,1-dinitroethane, 1,1-dinitropropane, and 2,2-dinitropropane) were measured for the cases of heavy confinement in thick-walled lead cylinders and Dremin's weak shell confinement. Shock-induced reaction times and failure wave velocities in decaying detonation waves were also measured and used in the Dremin-Trofimov model to calculate failure diameters of the unconfined liquids. The Dremin-Trofimov model was found to give good agreement with experiment when the Chapman-Jouguet (CJ) properties of the steady state detonation wave are accurately known.

CONTENTS

PREFACE ii

ACKNOWLEDGEMENT ii

SUMMARY iii

INTRODUCTION AND BACKGROUND 1

RESULTS DURING THE LAST REPORT PERIOD 4

REFERENCES 5

APPENDICES A, B, AND C ATTACHED

INTRODUCTION AND BACKGROUND

For fourteen years SRI has carried out a program of basic research for the Office of Naval Research into the relationship between detonation phenomena and chemical structure and kinetics, first with difluoraminoalkanes and later with dinitropropanes.

The overall objective of the program is to study the fundamental sensitivity properties of energetic organic compounds to define the minimum number of physical and chemical parameters needed to predict initiation and failure characteristics of high- and low-velocity detonations. Put in simple terms, our goal is to define the characteristics of a molecule that determine its degree of susceptibility to initiation and that establish its subsequent action in the detonation phase. Empirical tests have given only a series of relative sensitivity values and none of the test methods seemed to correlate with one another. Thus a worker has been forced to estimate roughly the extent of his problem by running small scale tests of a compound's sensitivity to impact, friction, spark, shock pressure, and thermal ignition. The test results were affected by the scale, the mechanics of the test, the perturbations introduced by the equipment, and a variety of phenomena unrelated to the inherent sensitivity characteristics of the compound being studied. Consequently, much important information was left undetected, such as failure diameter, ability to propagate, susceptibility to low-velocity detonation, and whether a detonation will be sustained in a medium when the quantities are larger than the few milligrams or grams used in small scale tests. Thus, the results were not useful to predict conditions beyond the scale of the tests because they may reflect only different paths of decomposition after the initial hot spot is induced by different modes of initiation. For example, an impact test may reflect the ease of thermal decomposition; the hot wire test may reflect vaporization and gas phase ignition; spark tests may reflect

ignitability in vapor phase; friction tests may reflect thermal decomposition characteristics.

Of the many available sensitivity tests, we have selected shock initiation and failure diameter of liquids for our basic studies, because these tests show under what conditions the liquids will undergo low- and high-velocity detonation (LVD and HVD). These tests are more reproducible, more homogeneous, and more susceptible to theoretical treatment than most sensitivity tests.

The explosive properties of a molecule are inherently related to its structure, which defines its energy, physical state, and ease of ignition. In a gross sense, the differences in sensitivity of RDX and TNT, of nitroglycerin and dinitrobutane are easy to distinguish. But what is not known is the contribution of various energy groupings to the overall sensitivity picture. Consequently, to avoid studying compounds that are unrelated in structure and in properties, we chose to study the isomers of compounds that contained important energetic groups, such as difluoroamino and nitro. To a first approximation then, the differences in detonation behavior can be related to chemical structure.

The results of this study on difluoroaminoalkanes were summarized in a report issued in 1970;^{1*} most of those results have subsequently been published.²⁻⁵ During the past five years, we have investigated the detonation sensitivity of isomeric dinitropropanes and other dinitroalkanes in three areas:

- (1) High-velocity detonation (HVD) phenomena, including gap tests for smooth shock reaction times, failure diameters, and shock temperature calculations.
- (2) Low-velocity detonation (LVD).
- (3) Kinetics of homogeneous gas-phase and liquid phase decomposition, including effects of high pressure on rate.

* References are numbered separately in the report and in the three manuscripts found in Appendix I.

This report summarizes the major efforts in HVD phenomena and kinetics of homogeneous gas and liquid phase decompositions of dinitroalkanes and is in the form of three manuscripts that have been or will shortly be submitted for publication.⁶ This is the last report to be issued on Contract N00014-70-C-0190. Although the ultimate objective of this program, prediction of detonation parameters from chemical structure and kinetics, has not been totally achieved, a large number of significant scientific advances were made in understanding the relation of structure to both detonation phenomena and chemical kinetics for these energetic compounds. This program has also discovered several important new effects of structure on detonation properties and chemistry, including the "alpha-hydrogen effect," the origins of which remain obscure and which deserves additional study.

This last report for this project consists of the following brief section on our results during the last report period followed by an appendix containing three manuscripts prepared from this research during the past 3 to 4 years.

RESULTS DURING THE LAST REPORT PERIOD

Much of the last report period from July to December 1975 was devoted to writing two manuscripts: (1) "Thermal Decomposition of 1,1- and 2,2-Dinitropropanes II. Liquid Phase," by Ross, Mill, and Kirshen; and (2) "Detonation Failure Diameter Studies of Four Liquid Nitroalkanes," by Tarver, Shaw, and Cowperthwaite. These appear in the Appendix along with a third manuscript, "Thermal Decomposition of Dinitropropanes I. Gas Phase," by Ross and Piszkiwicz.

Some experimental work was done with mixtures of isobutane or neopentane with NO_2 , the results of which are described in manuscript 1.

REFERENCES

1. M. E. Hill, D. S. Ross, R. Shaw, R. W. Woolfolk, T. Mill and L. B. Seely, "Sensitivity Fundamentals" Final Report, SRI Project 4051, ONR Contract No. Nonr 3760(00), May, 1970.
2. A. B. Amster and R. W. Woolfolk, "Initiation of Low Velocity Detonation," Bull. A.P.S. Series II, Vol. II, 766 (1966).
3. S. K. Brauman and M. E. Hill, "Kinetics and Mechanism of the Dehydrofluorination of 2,3-Bis(difluoramino)butane," J. Am. Chem. Soc., 89, 2131 (1967).
4. D. S. Ross, T. Mill, and M. E. Hill, "The Very Low Pressure Pyrolysis of NF Compounds, II - 1,2- and 2,2-Bis(difluoramino)propane," J. Am. Chem. Soc., 94, 8776 (1973).
5. B. O. Reese, L. B. Seely, Robert Shaw, and Derek Tegg, J. Chem. Eng. Data 15, 140 (1970).

Appendix A

THERMAL DECOMPOSITION OF 1,1- AND 2,2-DINITROPROPANE IN THE LIQUID PHASE

by

D. S. Ross, N. Kirshen and T. Mill

THERMAL DECOMPOSITION OF 1,1- AND 2,2-DINITROPROPANE IN THE LIQUID PHASE*

D. S. Ross, N. Kirshen and T. Mill

ABSTRACT

Thermal decomposition of neat, liquid 1,1-DNP at 1 and 1000 atm and 135-155°C gives over 90% propionic acid with small amounts of acetic acid. The reaction is accelerated by pressure and by added water. Rates of reaction are quite erratic with conversions ranging from 29% in 1.5 hours at 135° and 1000 atm to 10% in 21 hours at 155° and 1 atm. 2,2-DNP, in contrast, decomposed slowly at 165°C to give only acetone, NO and NO₂. Pressure retarded the reaction slightly. At 190°C 2,2-DNP had a half-life of 15 hours and gave with increasing conversion increasing amounts of acetic acid, CO₂, CO, and N₂O. The rate of formation of acetone remained nearly constant out to 90% conversion. Reactions of isobutane and neopentane with NO₂-N₂O₄ indicate that HNO₃ is an intermediate oxidizer in these reaction mixtures.

Possible mechanisms for these reactions are discussed.

Introduction and Background

Differences in sensitivity among different explosives are well known: nitroglycerine is much more prone to detonate on accidental impact than is TNT. Even among structurally similar explosive molecules, including isomers, differences in ease of detonation can be quite marked,

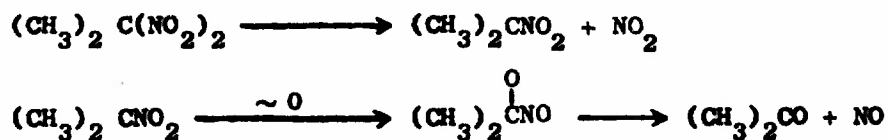
* This work was supported by the Office of Naval Research under Contract N00014-70-C-0190.

which indicates that initiation is a kinetically controlled process.

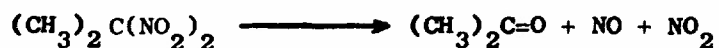
A comprehensive theory of sensitivity requires, among other things, that we understand how molecular structure affects sensitivity. One of the major obstacles to developing relations of this kind is lack of a well defined and agreed-upon test for sensitivity. In this laboratory, sensitivity has been measured by smooth-shock reaction time, by time-to-explosion, and by failure diameter. The widely used impact test is too complex and irreproducible from place to place to be of value in establishing basic structure-sensitivity relationships. Several years ago, we used these sensitivity tests together with rate measurements to show that smooth-shock reaction times paralleled the rates of loss of HF from vicinally-substituted difluoroaminoalkane isomers while LVD gap sensitivity paralleled the C-N bond strengths, being most sensitive for gem-NF₂ isomers.¹

We have now examined the sensitivity and kinetic characteristics of several isomeric dinitropropanes. Sensitivity studies, including reaction-time measurements and failure diameter, are reported elsewhere in detail² and show that sensitivity changes with structure. Specifically, the presence of hydrogen alpha to the nitro group(s) significantly reduces smooth-shock and explosion times. Dinitropropanes having no α hydrogens show no change in sensitivity with increasing pressure. The origins of this so-called " α -hydrogen effect" remain obscure, but the effect is certainly real.

In a previous paper,³ we reported the results of very low pressure pyrolysis (VLPP) of several dinitropropanes. That work, along with the work of others,⁴ established the C-N bond strength in gem-dinitroalkanes as about 47 kcal/mole. These compounds decompose in the gas phase through initial C-N scission, followed by rearrangement and loss of NO. Using 2,2-DNP for the example

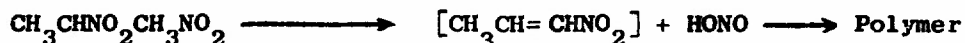


The overall reaction is then



1,1-DNP decomposes to give propionaldehyde, NO, and NO₂ by a similar process.

In contrast, nongeminate substituted nitroalkanes, including both mono- and dinitro compounds, having C-N bond strengths of 59 kcal/mole decompose via a lower energy cyclic HONO elimination.



To gain additional insight into the kinetic processes associated with initiation of detonation, we investigated the rates and products of thermal decomposition of neat liquid 1,1- and 2,2-dinitropropanes (1,1-DNP and 2,2-DNP) at 140-190°C and 1-3000 atm. These decomposition studies were made under similar conditions of pressure and temperature to those used for thermal explosion time measurements⁵ but not such severe conditions as those found in shock initiation experiments (500-1000°K and 100,000 atm). Thermal explosion studies provide useful overall kinetics, whereas thermal decomposition studies such as those described here can provide information about the elementary steps and products prior to thermal explosion.

The physical properties of these two isomeric DNPs are summarized in Table 1.

Table 1

PHYSICAL AND THERMODYNAMIC PROPERTIES OF 1,1-DNP AND 2,2-DNP
(from ref. 6)

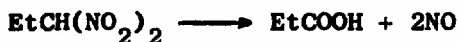
Measured Physical and Thermodynamic Properties at 60°C	1,1-DNP $\text{CH}(\text{NO}_2)_2\text{CH}_2\text{CH}_3$	2,2-DNP $\text{CH}_2\text{C}(\text{NO}_2)_2\text{CH}_3$
Molecular weight	134.1	134.1
Density/(g/ml)	1.201 ± 0.01	1.221 ± 0.01
Coeff. of Exp/(K ⁻¹)	(-1.0 ± 0.1) × 10 ⁻³	(-0.98 ± 0.1) × 10 ⁻³
Sound Speed/(mm/μsec)	1.33 ± 0.05	1.24 ± 0.05
Heat of Formation/(cal/g)	-283 ± 20	-300 ± 20

Results

1,1-DNP

Some preliminary experiments on neat 1,1-DNP indicated that at 1 atm and 150-155°C, 1,1-DNP decomposed slowly, but considerably faster than predicted from gas phase kinetic parameters.³ Thus the calculated gas phase rate at 155°C is about 0.001%/hr whereas the observed liquid phase rate is about ~1%/hr.

More detailed studies showed that during the very initial stages of decomposition at both 1 atm and 1000 atm, several different products are formed. But at high conversions, 1,1-DNP invariably produces over ~90% yields of propionic acid under all conditions tried from 135-165°C and from 1-1000 atm. Small, variable amounts of acetic acid were found as well. The major overall process for decomposition of neat 1,1-DNP appears to be



The rate of decomposition of 1,1-DNP was found to be erratic. A series of experiments at 135 and 145° and 1000 atm, summarized in Table 2, show that the reaction is complete in less than 24 hours with formation of both acetic and propionic acids in a ratio of 1:9. At much shorter times, conversions are low, but variable, ranging from none at 1.5 hours to 75% in 6 hours. A significant effect of water, added in 3 wt%, was found: 29% of 1,1-DNP decomposed in 1.5 hours compared with no detectable decomposition in a similar sample without added water.

The erratic kinetic behavior of 1,1-DNP is more readily seen in the results at 145°C where conversions of 1 to 68% were found in similar samples heated for 0.5 to 1.5 hours. Product analyses on some of these samples showed the presence of both acetic and propionic acids in proportions varying from 1:23 for run 59c to 1:4 for run 59b. One sample of 1,1-DNP, purified by gas chromatography, (in run 59c) had about half the rate of decomposition of an unpurified control; the difference is well within the error limit but shows that impurities normally present in 1,1-DNP have no major effect on its rate of decomposition.

Table 2

DECOMPOSITION OF 1,1-DNP AT 1000 ATM

Run No.	Temp. (°C)	Time (hr)	Conversion (%)	Products, wt %	
				MeCO ₂ H	EtCO ₂ H
58b	135	1.5	0	--	--
60b	135	1.5	0	--	--
60a ^a	135	1.5	29	--	29 ^b
58 ^d	135	3	8	--	8 ^b
58d	135	6	75	--	--
57a	135	24	99	10	86
55	145	0.5	~ 0.5	--	--
59b	145	0.67	68	14	54
59c ^c	145	0.67	24	1	23
56	145	1.0	1	--	--
59a	145	1.2	31	4	27

^a Water added in 3 wt %.

^b Unresolved mixture of acids.

^c 1,1-DNP purified by glc.

A conventional first-order plot of log [DNP] versus time (not shown) gave a markedly downward curved plot indicative of autocatalysis.

At 1000 atm and 155°C decompositions are unpredictable, sometimes proceeding smoothly for up to 125 minutes and at other times exploding after only 25 minutes. Similarly, the rates of decomposition of 1,1-DNP at 155°C, which are about 0.5-1%/hr at 1 atm, are as much as 4%/hr in one hour at 1000 atm. Longer heating at 155°C and 1000 atm invariably produces explosion or charring. Products are the same as found at 135°. Table 3 summarizes these results.

Table 3

EFFECT OF TEMPERATURE AND PRESSURE ON THE DECOMPOSITION OF 1,1-DNP

<u>Experiment</u>	<u>Time (hr)</u>	<u>Temp. (°C)</u>	<u>Pressure (atm)</u>	<u>Conversion (%)</u>
6,7,8	21	155	1	10
11	17	155	1000-200 ^a	99
44	1	155	1000	4
46	2	155	1000	1
56	1	155	1000	1.6
50,51	2	155	1000	exploded
9	21	165	1 ^b	99
10	21	165	20	90

^a Pressure dropped from 1000 to 200 atm during experiment.

^b Run in a sealed Pyrex tube.

The experimental difficulties of handling these materials quantitatively at high pressures, coupled with the erratic character of the reaction, particularly at higher temperatures, prevents us from developing any detailed understanding of the processes taking place. The results point to the major process being an ionic, oxidative hydrolysis promoted by increased pressure.

2,2-DNP

Absence of reactive α -hydrogens in 2,2-DNP suggests that it should be more stable in the liquid phase than 1,1-DNP. Experiments at 165°C at 1 atm and 1000 atm summarized in Table 4 confirm this. No significant decomposition is noted until 2,2-DNP (6.89M) is heated at temperatures of 165°C for at least 24 hours. The observed rate of 0.02-0.007M/hr agrees closely with the rate predicted from gas phase measurements;³ pressure has only a small retarding effect while added water has no effect on rate. Analyses of reaction mixtures show acetone as the single significant organic product.

Table 4

DECOMPOSITION OF 2,2-DNP AT 165°C

<u>Experiment No.</u>	<u>Time (hr)</u>	<u>Pressure (atm)</u>	<u>Conversion (%)</u>	<u>Rate M/hr</u>
1 ^a	24	1	5	0.014
2 ^b	24	1	3	0.009
3 ^a	24	1000	2	0.006
4 ^a	166	1000	14	0.006

^aFEP tubing

^bPyrex

At 1000 atm the initial rate of decomposition of 2,2-DNP at 165°C follows apparent first-order kinetics based on three time points ($t = 0, 24, \text{ and } 166$ hours) with a rate constant of $2.3 \times 10^{-7} \text{ sec}^{-1}$. This rate is about one-half as fast as at 1 atm in FEP tubing and about half the rate predicted from gas phase measurements ($k_1 = 4.7 \times 10^{-7} \text{ sec}^{-1}$).³ In each case, acetone is the only major product detected; although nitrogen oxides were found in small amounts, most were lost by diffusion through the FEP tubes.

A more detailed study of the thermal decomposition of liquid 2,2-DNP was carried out at 190°C and 1.2 atm in Pyrex tubes (autogenous

pressure of 2,2-DNP) at 2 to 93% conversions with detailed product analyses. (At 190°C and 1 atm, about 5% of the initial DNP is in the gas phase; in longer runs the total final pressure in the tubes was 10 to 20 atm).

The major initial decomposition products were acetone, CO₂, HOAc, and NO; later, increasing amounts of N₂, N₂O, and CO were also observed but in lesser quantities. NO disappeared in a short time and NO₂ is notable by its absence. Table 5 summarizes the results.

Inspection of C, H, N, and O mass balances from products showed a significant deficit in the H and O values, but this deficiency is reasonably accounted for by assuming water to be a major product. Thus, in Table 5 mass balances in the longer runs are satisfactory, except for a carbon deficit of 20% in the 39-hour runs.

The products appear to fall into two classes: (1) primary products including acetone and NO, which result from simple unimolecular decomposition of 2,2-DNP and are the only products observed at lower temperatures in neat liquid and in the gas phase; (2) secondary products including acetic acid, CO, CO₂, N₂, and N₂O, which are obviously the products of oxidation-reduction processes in which carbon is oxidized and nitrogen is reduced.

There is more CO₂ than acetic acid by a factor of over two. Thus the methyl carbon lost in the formation of the acetic acid is not the only source of CO₂, and some must also be formed by direct oxidation of 2,2-DNP itself, or of its daughter two- and three-carbon fragments. Further oxidation of acetic acid to CO₂ is possible, but the data do not indicate this.

Rate data for disappearance of 2,2-DNP and appearance of products at 190° are shown in Figures 1a and 1b*. The initial rate

* It is convenient to analyze the data by considering the apparent first order rate constants. They are effectively the average of rates of reactant consumption and product formation over a given interval, normalized to unit 2,2-DNP concentration within that interval.

Table 5

**THERMAL DECOMPOSITION OF 2,2-DNP
at 190°C**

Reaction Period (hr)	Conversion ^b (%)	Initial 2,2-DNP (μ-moles)	Products (μ-moles)						Mass Balances ^a (%)		
			CO	CO ₂	Acetone	Acetic Acid	N ₂	N ₂ O	NO	C	N
1	2-3	960	6 ^c	10	20	5-10	4	2	18	--	--
5	2-3	900	6 ^c	d	15	trace	9	12	7	--	--
15	13	1050	28	106	65	e	91	44	d	97	100
23	15	930	27	88	40	e	86	30	d	94	98
39	50	860	3-4	270	160	73	260	96	d	86	91
	43	790	45	260	150	55	225	87	d	93	97
	61	1000	60	442	250	180	430	170	d	92	98
	63	930	85	388	220	160	400	150	d	89	96
	91	880	80	495	290	240	567	171	d	82	93
	93	880	100	510	280	240	577	179	d	79	92

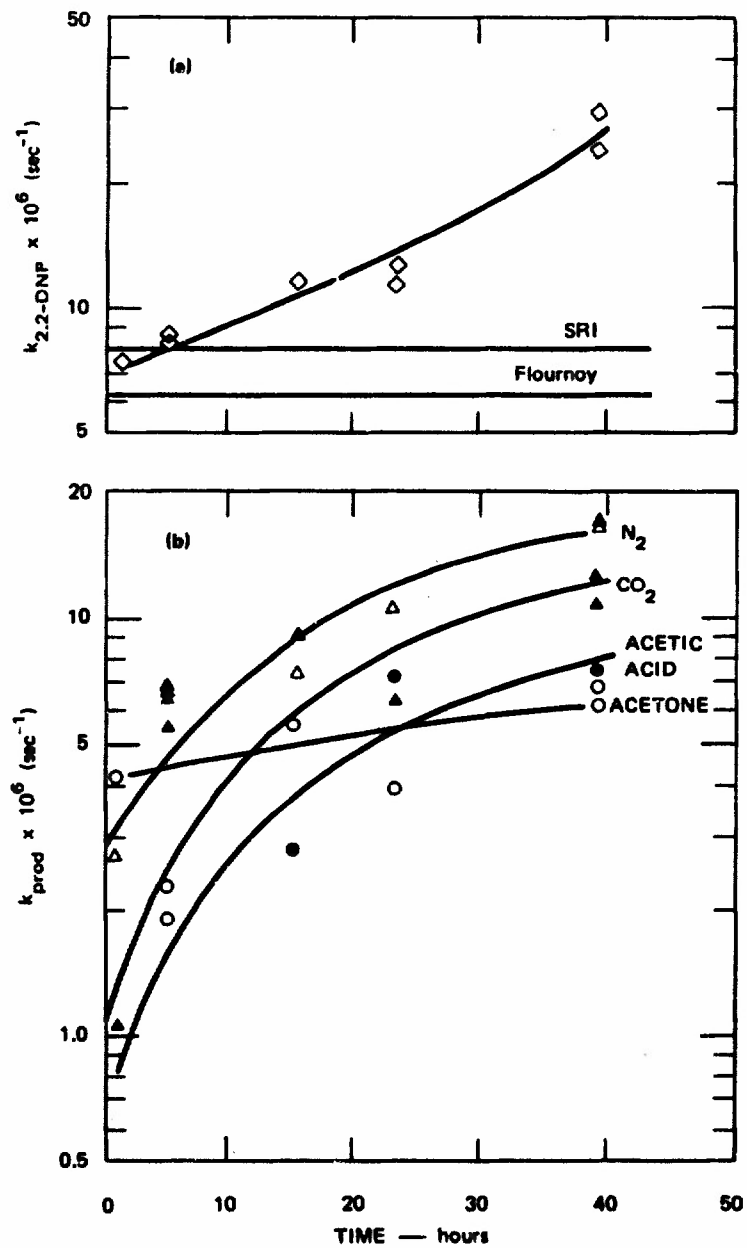
^a At low conversions mass balances are not significant.

^b Estimate from the relation $DNP = Acetone + HOAc + (CO + CO_2)/3$.

^c Estimated.

^d None detected.

^e Not measured.



TA-8828-87R

FIGURE 1 AVERAGE FIRST ORDER RATE CONSTANT FOR (a) DISAPPEARANCE OF 2,2-DNP AT 190°C, \diamond ; (b) APPEARANCE OF PRODUCTS AT 190°C, \triangle - N_2 , \triangle - CO_2 , \bullet -ACETIC ACID, \circ -ACETONE

constant is about $8 \cdot 10^{-6}$ sec, very close to the rate constant that is calculated from gas phase kinetic parameters.³ The difference in rate between gas phase and liquid phase is well within the error limit of the calculation.

Also shown in Figure 1a is the rate constant at 190° derived from the Arrhenius expression for the gas phase reaction studies by Flournoy.⁷ The close agreement with results from the present study are apparent. Although the initial rate of decomposition of 2,2-DNP is nearly the same as the gas phase rate, after a short while, the rate begins to increase autocatalytically.

The product formation rates in Figure 1b point out more clearly the nature of the autocatalysis. Acetone is produced at a constant rate throughout the reaction out to 39 hours, or to better than 90% reaction. This reaction also produces NO and NO₂, which must be responsible for the oxidation-reduction sequence producing ultimately CO₂, N₂, and acetic acid. Figure 1b shows that the rate constants for formation of these products increase with time. Thus, the NO_x produced initially through reaction (1) oxidizes 2,2-DNP and, in turn, the oxidized DNP produces more NO_x.

The results of experiments at 1, 1000, 2000, and 3000 atm at 190° and 210°C, summarized in Table 6, show that the rate of decomposition of 2,2-DNP is not significantly affected by the application of high pressure at 190°C nor by addition of NO₂ or O₂.

The effect of applied pressure on the process does, however, become significant at 210°C. Whereas, conversions of 10-30% are found near 1 atm, conversions are ~99% complete at 2-3000 atm, producing only a brown residue in the tubes. Possibly conversions at high pressure are overstated because of permeability of the FEP tubes at these temperatures; however, judging from the appearance of the residues, pressure markedly affects the reaction course.

Table 6

EFFECT OF PRESSURE, O₂ AND NO₂ ON DECOMPOSITION OF 2,2-DNP
AT 190 AND 210°C FOR 1 HOUR

Experiment No./Addend	Temperature (°C)	Pressure ^{a, b} (atm)	% Conversion ^c	Rate, (M/hr) ^g
1	190	1	2,3	0.20
2	190 ^d	1	12,16	1.1
3	190	1000	13,17,19,13	1.2
4/O ₂ ^e	190	1	2,3	0.2
5/O ₂ ^f	190	1000	10,19	1.1
6/NO ₂ ^e	190	1	2,3	0.2
7/NO ₂ ^f	190	1000	19,10,12	1.1
8	210	1	22,10,33	1.7
9	210	2000	> 99	8.05
10	210	3000	> 99	8.05

^a Samples run at 1 atm contained 100 mg (0.75 mmole) of 2,2-DNP in Pyrex tubes.

^b Samples run at > 1000 atm contained 15 mg (0.11 mmole) sealed in FEP tubes.

^c Conversions for replicate samples.

^d Run FEP tubing.

^e Added 20-30 μmole.

^f Added 0.2 μmole.

^g Averaged for replicate samples and based on 8.05M concentration for neat 2,2-DNP at 190°.

Reactions of NO₂ with Hydrocarbons

Both kinetic and product data point to formation of NO₂ in the initial step. To gain some additional insight into the secondary reactions of NO₂ with the parent compound, we examined briefly the reactions of NO₂ and N₂O₄, the likely form of NO₂ at high pressures, with isobutane and neopentane. These compounds were chosen for study because of their simplicity and markedly different reactivity toward radical species like NO₂.⁸ Both gas phase and condensed phase reactions were examined in which the proportion of NO₂ to N₂O₄ was varied by adjusting the total amount of N₂O₄ added initially and using equilibria values of Gurney⁹ to calculate the quantities of monomer and dimer. Results are summarized in Table 7.

Experiments 1-6 show the effect of an increase in initial concentrations of N₂O₄, and of a change from an all-gas-phase system to one in which there are both gas and condensed phases on the conversion of isobutane. The reaction rate increases substantially when the system contains condensed N₂O₄. Experiment 10 with neopentane showed no reaction under conditions where isobutane was totally consumed (experiment 3).

The conversion is not a function of the NO₂ concentration, but seems to be closely associated with the initial quantity of N₂O₄. Experiments 2 and 5, with about the same initial quantities of NO₂, but much different quantities of N₂O₄, show that the rate is faster in the condensed phase (largely N₂O₄) than in the gas phase by about a factor of eight. The increase in conversion in experiments 3-6 parallels the increased reaction time and suggests simple pseudo first-order behavior.

Experiment 7 shows the effect of added NO. Here the quantity of N₂O₄, estimated as described, is substantially lowered through the reaction



The rate in this case appears to be similar to that for experiment 2, a gas-phase run with a comparable quantity of N₂O₄ but a significantly larger quantity of NO₂.

Table 7

REACTION OF ISOBUTANE AND NEOPENTANE WITH $\text{NO}_2/\text{N}_2\text{O}_4$ AT 100 AND 130 C^a

Expt. No.	Reaction Temp. (C)	Time (min)	Initial Stoichiometric Quantity of N_2O_4 (μmoles)	Pressure at Reaction Temp. b,c (atm)	Phases Present at Reaction Temperature	Addend (μmoles)	Calculated N_2O_4 at Reaction Temp. b,d (μmoles)	Calculated NO_2 at Reaction Temp. b,d (μmoles)	% Conversion ^e Hydrocarbon
ISOBUTANE									
1	100	60	205	9.6	gas	none	98	214	25
2	"	"	464	19.7	gas	none	281	361	52
3	"	"	2418	20.0	liquid + gas	none	2260	~ 315	99 ⁺
4	"	15	"	"	"	"	"	"	73
5	"	8	"	"	"	"	"	"	54
6	"	4	"	"	"	"	"	"	24
7	"	60	1210	~ 18 ^f	"	NO(1807)	~ 300 ^f	Probably 10 ^f	60
8	130	"	205	11.7	gas	none	55	299	79
9	130	"	205	~ 22 ^f	gas	NO(315)	~ 55 ^f	~ 300 ^f	77
NEOPENTANE									
10	100	60	2418	22	liquid + gas	none	2260	~ 315	< 0.1
11	100	60	2418	22	"	H ₂ O(50)	2260	315	25

^a Reactions carried out in sealed 1-ml pyrex breakseal tubes with 125 μmoles hydrocarbon present initially.

^b Calculated for the gas phase by extrapolation from lower temperature equilibrium data; F. Verhoek and F. Daniels, J. Am. Chem. Soc., 53, 1250 (1931).

^c Calculated from the vapor pressure of N_2O_4 ; Matheson Gas Data Book, 4th Ed. (The Matheson Co., Inc., East Rutherford, N. J. (1966)).

^d From our extrapolation of Vosper's data; A. Vosper, J. Chem. Soc., 2191 (1970).

^e Each run was performed at least in duplicate, and the results shown here are the averages. The results were reproducible to better than $\pm 5\%$.

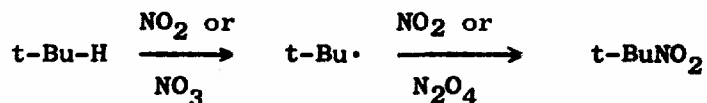
^f From our extrapolation of Vosper's data; A. Vosper, J. Chem. Soc., (A), 1759 (1966).

^g Vosper has shown that in these systems containing condensed $\text{NO}/\text{NO}_2/\text{N}_2\text{O}_4$, little NO_2 exists in both the gas and liquid phases. A. Vosper, J. Chem. Soc., (A), 1589 (1971).

^h Vosper has shown that in these systems containing condensed $\text{NO}/\text{NO}_2/\text{N}_2\text{O}_4$, little NO_2 exists in both the gas and liquid phases. A. Vosper, J. Chem. Soc., (A), 1589 (1971).

Finally, the experiments at 130° (8, 9) show that the addition of NO has no effect under conditions where there is no liquid phase and little NO-NO₂ association.

These experiments yielded several products by glc analysis; however, the only product identified was 2-nitro-2-methylpropane. It was the major product found in all experiments, in quantities equal to 15-20% of the consumed isobutane. Undoubtedly, 2-nitro-2-methylpropane forms via the t-Bu radical



The same process should also yield the corresponding nitrite; however, none was found. From the gas phase unimolecular rate parameters for the thermal decomposition of n-butyl nitrite¹⁰ we can estimate that thermal decomposition of t-butyl nitrite would be far too slow to account for its absence. It is possible that quenching the reaction mixture in methanol converted the nitrite to t-butanol through a transesterification process. However, we found no evidence for that alcohol.

Gaseous products included CO₂, CO, N₂O, and N₂, the amounts of which account for only a few percent of the carbon in the consumed isobutane. Traces of methyl nitrite were observed in the low conversion runs. Its thermal stability should be similar to that for t-butyl nitrite, and the fact that it is observed only early in the reaction period suggests that there is another possible sink for nitrites in the reaction mixture.

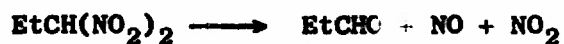
Neopentane was found to react with NO₂-N₂O₄ only in the presence of water. Products could not be characterized.

Discussion

The thermal decomposition of liquid 1,1-DNP is about 100 times as fast as that of 2,2-DNP at 150-160°C. This observation alone alerts us to the likelihood that 1,1-DNP is not decomposing to any significant extent by simple C-N scission because the C-N bond strengths in 1,1- and 2,2-DNP are closely similar.³ The catalytic effect of water on the rate of decomposition of 1,1-DNP confirms the assumption drawn from the rate data that the decomposition of 1,1-DNP is an ionic process similar to that observed in aqueous acid at lower temperatures where Kamlet found that terminal dinitroalkanes gave carboxylic acids.¹¹

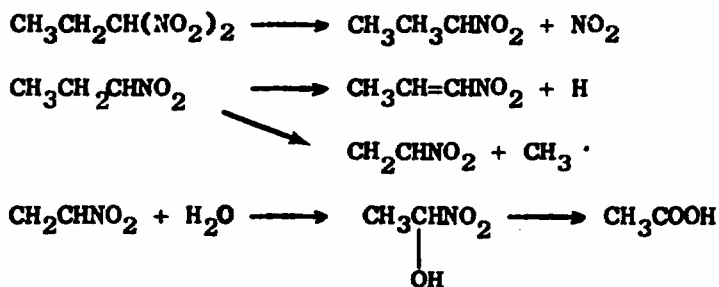
On one point the data are ambiguous: acetic acid is formed in small but variable amounts in most runs but cannot be a product from the same intermediates leading to formation of propionic acid. Formation of acetic acid from 1,1-DNP requires cleavage of C-C bonds and extensive reorganization, suggesting the possibility that there are parallel paths of decomposition that have different temperature dependencies. Under explosive or detonation conditions only one higher enthalpy pathway will be important. The idea of parallel paths for decomposition is reaffirmed by the observation that water has no effect on time-to-explosion of 1,1-DNP at 195°C,⁵ in contrast to its effect on thermal decompositions at 135°C.

Although we cannot account in detail for the decomposition, the facts are consistent with a scheme involving initial slow C-N scission to form oxygenated intermediates such as propionaldehyde.



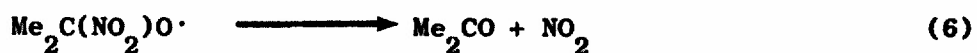
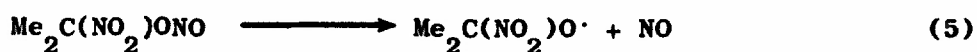
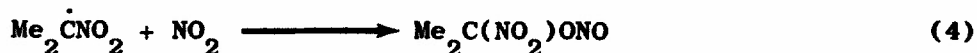
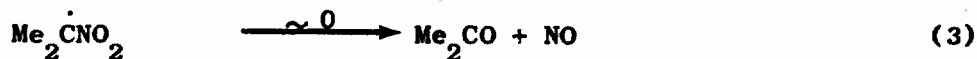
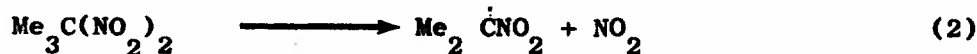
and nitrogen oxides. Further oxidative reactions of NO₂ and/or NO to form water (via HNO₂) then promote the conversion of 1,1-DNP to propionic acid by an ionic route. Since 1,1-DNP is itself acidic, one might consider the autocatalytic role for 1,1-DNP in the "Kamlet" reaction.

Acetic acid could arise from two sources: cleavage of nitropropylene or (more likely) oxidative hydrolysis of nitroethylene.



Lack of effect of water on time-to-explosion⁵ suggests that oxidative hydrolysis no longer competes with other exothermic reactions that contribute to the global kinetics observed in this kind of experiment. However, efforts to analyze products at these higher temperatures, looking for evidence of incursion of other reaction paths, was unsuccessful owing to rapid onset of explosive decomposition.

Decomposition of 2,2-DNP is appreciably simpler. Both kinetic and product data point to a mechanism for decomposition that involves initial C-N scission, followed by rearrangement or recombination and O-N scission³



Both schemes give the same products. Scheme (2,3) almost certainly describes the gas phase process at low pressure where recombination is unlikely, whereas scheme (2,4,5,6) may be important in solution where cage combination would be favored, particularly at higher pressures. As long as reaction (2) is slow and rate controlling, the rate law and observed rate constant remain the same.

The marked accelerating effect of applied pressure on decomposition of 1,1-DNP but not of 2,2-DNP is further evidence for very different decomposition pathways for the two isomers. The effect of applied pressure on reaction rate may be exerted on both the physical properties of the medium (as for example an increase in viscosity) and on the chemical properties of the transition state (as expressed in ΔV^\ddagger , the volume of activation). A detailed analysis of pressure effects on rates is given by Neumann.¹² The change in rate constant for a unimolecular process with change in pressure is given by

$$\log (k_1'/k_2') = \Delta V_{\text{obs}}^\ddagger [p_{21} - p_{11}] / 2.303 RT \quad (7)$$

where $R = 82.07 \text{ cm}^3/\text{mole}$ and p is in atm.

Measurements of pressure effects on reaction rates are necessarily composites of both chemical and viscosity effects; both must contribute to $\Delta V_{\text{obs}}^\ddagger$ in reversible one-bond scissions.

Experiments with several different reversible homolytic one-bond scission reactions similar to C-N cleavage in 1,1- or 2,2-DNP give $\Delta V_{\text{obs}}^\ddagger = 10\text{-}15 \text{ cm}^3/\text{mole}$:¹² pressure retards the bond cleavage. The major portion of this retardation arises from effects of pressure on elementary steps following the slow, rate-controlling step k_1' .

Ionic dissociation processes are accelerated by pressure ($-\Delta V^\ddagger$) and often have large $\Delta V_{\text{obs}}^\ddagger$ owing to electrostriction of solvent by ions.¹¹ Decomposition of 1,1-DNP at 151°C is accelerated by pressure and shows a positive rate effect as large as 5 for a positive change in pressure of 1000 atm. This rate factor corresponds to ΔV^\ddagger of $-56 \text{ cm}^3/\text{mole}$, which is consistent with a complex ionic mechanism but surprisingly high in comparison with other values reported for ionic reactions.¹²

From equation (7) we can calculate the effect of pressure on the cleavage of the C-N bond in 2,2-DNP at 165°C, assuming $\Delta V_{\text{obs}}^\ddagger = 15 \text{ cm}^3/\text{mole}$. Table 8 shows that a change in pressure of 1000 atm decreases the relative rate by a factor of only 2, very close to the observed effect.

Table 8 also shows that if we increase the pressure to 5000 atm, k_{obs} is reduced to 10% of the original value. Thus a further test of the proposed mechanism for decomposition of 2,2-DNP would be to evaluate $\Delta V_{obs}^{\ddagger}$ accurately over a wider range of pressure.

Table 8

CALCULATED EFFECT OF PRESSURE ON RATE OF DECOMPOSITION
OF 2,2-DNP AT 165°C FOR $\Delta V^{\ddagger} = 15 \text{ cm}^3/\text{mole}$

<u>Pressure (atm)</u>	<u>Relative^a Rate Constant k_{obs}</u>
1	1
1000	0.66
5000	0.12
10,000	0.015
30,000	3.6×10^{-6}

^aCalculated using equation (7).

Interestingly, global kinetic data for decomposition of 1,1- and 2,2-DNP, derived from time-to-explosion measurements, are in the same directions as for isothermal experiments described here.⁵ On the assumption that times-to-explosion are inversely related to first-order rate constants for initial cleavage of some bond, we can readily calculate $\Delta V_{obs}^{\ddagger}$ for 1,1-DNP and 2,2-DNP. Results are shown in Table 9. The values of ΔV^{\ddagger} are considerably smaller than those calculated from isothermal decomposition data over a much smaller range of pressure.

Since time-to-explosion basically measures the rate of heat release, a complex multistep process, the poor agreement between values of ΔV^{\ddagger} calculated in Table 9 and those derived from isothermal data are hardly surprising. However, the similar directions of pressure effects, although possibly adventitious, very likely reflect some basically common mechanism being observed by two different techniques.

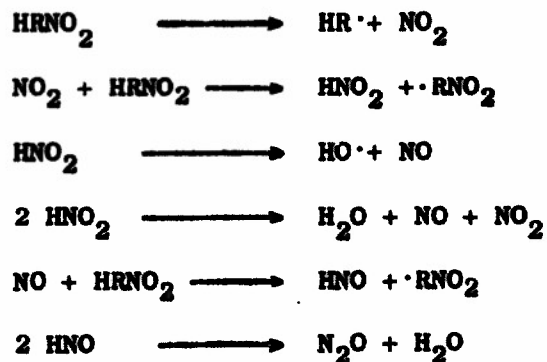
Table 9

TIMES TO EXPLOSION AND ΔV^\ddagger FOR
1,1- AND 2,2-DNP

<u>Pressure</u> (atm)	<u>Temp.</u> (°C)	<u>Time</u> (sec)	<u>k_{rel}</u>	<u>ΔV^\ddagger^a</u> (cm ³ /mole)
1,1-DNP				
1,000	195	100	0.03	-15
10,000	195	3	1.0	
2,2-DNP				
10,000	267	22	1.0	+ 1.5
50,000	267	84	0.24	
10,000	306	4	1.0	+1.9
50,000	306	20	0.2	

^aCalculated from equation (7).

Now let us consider the high conversion experiments with 2,2-DNP where extensive oxidation and cleavage of the carbon chain occurs. From the standpoint of initiation of detonation, these reactions are of greatest importance because, unlike the initial C-N homolysis, these reactions are exothermic processes that contribute to self-heating and ultimately to explosion or detonation. The first oxidizing species formed is NO₂ but it is rapidly reduced to NO, N₂O, and N₂ through a series of reactions with (probably) the parent molecule. Data on reactions of this kind are scanty but suggest several schemes by which these reductions may be effected. One such scheme is



Although each step in the sequence seems well established,¹³ the scheme must be regarded as speculative as applied to this system and is intended only to be illustrative of possible routes to final products.

The brief investigation of the reactions of isobutane and neopentane and $\text{NO}_2/\text{N}_2\text{O}_4(\text{NO}_x)$ indicate how unexpected complications arise in reactions of NO_2 and organic compounds. The markedly more rapid rate of reaction of isobutane with liquid N_2O_4 , as compared to the rate with NO_2 alone, is inconsistent with the simple explanation that H-atom transfer to NO_2 is the initial step in all cases, especially since the rate is undiminished in the presence of NO , an efficient scavenger of NO_2 under these conditions. The inertness of neopentane under the same conditions in liquid N_2O_4 is best explained by the requirement for a reactive tertiary hydrogen in the initial step, but the nature of this step remains unknown. Both radical and carbonium ion intermediates could give methyl nitropropane and the complex mixture that accompanies it.

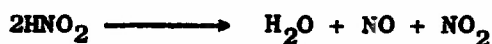
These data seem unequivocal on one point: the inertness of neopentane shows that the reactive species NO_3 generated via the O-bridge dimer of N_2O_4 cannot play a significant role in this process. All the information on NO_3 points to it being a reactive species forming a strong (101 kcal/mol) O-H bond by H-atom transfer from hydrocarbons and it is therefore expected to be somewhat unselective in attacking different CH bonds.¹⁴ For example, the reactive oxy radical t-BuO \cdot (104 kcal/mol OH bond) shows a tertiary/primary selectivity factor of 5/1 for these same two hydrocarbons at 100°.⁸ Our data show a selectivity factor of at least 1000/1 in this reaction mixture, which can only be accounted for by an unusually selective species such as NO_2 .

The significant rate of decomposition of neopentane of addition of water indicates that water in some way accelerates these reactions. And since water is a redox product of the thermal decomposition of nitroalkanes, an autocatalytic scheme seems likely.

It is tempting to suggest the following scheme for the thermal decomposition of nitroalkanes themselves, or of mixtures of alkanes and $\text{NO}_2(\text{N}_2\text{O}_4)$, based on the known hydrolysis of N_2O_4 ¹⁵ and the potent oxidizing capacity of nitric acid.¹⁶ First, Carberry¹⁵ states that molecular N_2O_4 reacts with water, while NO_2 does not react at all under typical hydrolytic conditions. Thus



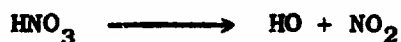
The nitrous acid formed is unstable under the prevailing conditions,



and the net reaction is



Nitric acid thermally decomposes to yield OH radical



which then reacts with hydrocarbon (or nitroalkane) RH,



This scheme explains the reaction of neopentane with N_2O_4 /water mixtures, and why the rate of reaction of isobutane/ N_2O_4 apparently is dependent on the concentration of N_2O_4 and not NO_2 .

If $\text{R}\cdot$ is $\cdot\text{C}-\text{C}-\text{NO}_2$, then loss of NO_2 by beta scission leads to a chain reaction.

Experimental

Chemicals--Samples of 1,1-DNP and 2,2-DNP were supplied by Aerojet-General Corporation. Gas chromatographic (glc) analyses showed only trace amounts of impurities. Compounds were stored in polyurethane containers to guard against explosion; no explosion was ever observed.

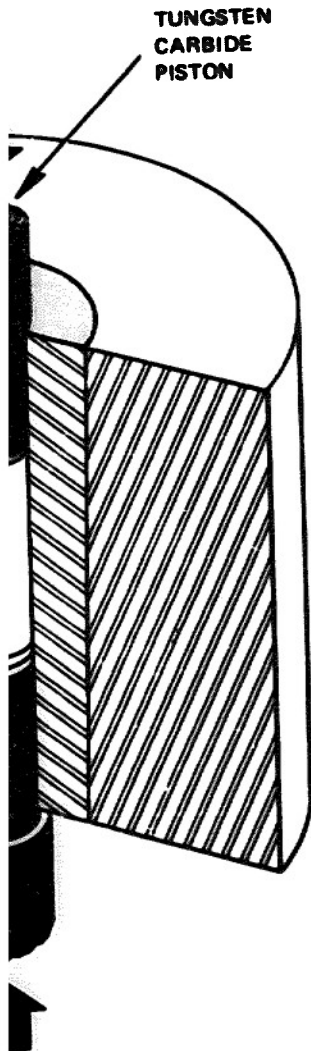
Reaction Procedure--We have developed an experimental procedure that provides a reliable way to heat small samples at 1000-3000 atm pressure and to 160°C and to recover the contents with only partial losses of gaseous products but with nearly quantitative recovery of liquid products. Thirty-microliter samples of DNP are placed in FEP tubing (5 mm I.D. by 10 mm), frozen, degassed, refrozen, and sealed under vacuum using a heat gun. With undegassed samples, extensive carbonization or complete rupture of the tubes invariably occurred in a few minutes at 140°C. When air was removed, the problem disappeared.

Sealed sample tubes were placed in the preheated pressure system described before and brought to pressure using a hydraulic hand pump. On completion of the heating period, the pressure was released, the tubes were quickly removed, cooled, and then cut open. The contents were mixed thoroughly with a weighed amount of benzyl alcohol, which served as an internal standard for glc. Glc analyses were carried out on a 10-foot by 1/4-inch 10% Ucon silicone column at 100°, except for glc-ms (mass spectrometry) where a 10-foot by 1/8-inch 1% silicone column was used.

A few samples were opened inside a vacuum line using a stopcock fitted with a thin wedge of razor blade, and gases were removed and analyzed by gas-phase ir.

Tubes are weighed before and after heating. In a few cases some weight loss was found, but most experiments at high pressure gave nearly quantitative retention of liquid reactant and products, the losses being associated with diffusion of NO_x through the FEP tubing.

Apparatus-All experiments were run in a piston-cylinder apparatus, shown in Figure 2, wrapped with a heating tape, and holding a sample fitting Teflon cup. The cup, filled with GE 7-55 silicone fluid, serves as both a pressure and temperature transmitting medium. The temperature of the assembly was controlled by a Westinghouse temperature controller and monitored continuously with a thermocouple and recorder.



TUNGSTEN
CARBIDE
PISTON

TA-8525-70

PISTON ASSEMBLY

REFERENCES

1. M. E. Hill, D. S. Ross, R. Shaw, R. W. Woolfolk, T. Mill and L. B. Seely, "Sensitivity Fundamentals" Final Report, SRI Project 4051, ONR Contract No. Nonr 3760(00), May, 1970.
2. C. M. Tarver, R. Shaw, and M. Cowperthwaite, *J. Chem. Phys.*, in press.
3. D. S. Ross and L. W. Piszkiwicz, "Very Low Pressure Pyrolysis of Dinitropropanes," manuscript submitted for publication.
4. G. M. Nazin, G. B. Manelis and F. I. Dubovitskii, *Izvest. Akad. Nauk.*, 374, 2494 (1968).
5. M. E. Hill, T. Mill, D. S. Ross, R. Shaw and R. W. Woolfolk, "Sensitivity Fundamentals," Technical Progress Report 73-1 (Semiannual), SRI Project 8525, ONR Contract No. N00014-70-C-0190, March, 1973.
6. M. E. Hill, T. Mill, D. S. Ross, R. Shaw, R. W. Woolfolk and C. Tarver, "Sensitivity Fundamentals," Technical Progress Report 73-2 (Semiannual), SRI Project 8525, ONR Contract No. N00014-70-C-0190, October, 1973.
7. J. Fluornoy, *J. Chem. Phys.*, 36, 1107 (1962).
8. D. G. Hendry, T. Mill, L. Piszkiwicz, J. A. Howard, and H. K. Eigenmann, *J. Phys. Chem. Ref. Data*, 3, 937 (1974).
9. A. Vosper, *J. Chem. Soc.*, A, 2191 (1970).
10. The "best" estimate gives $\log k = 16.8 - 41.5/\theta$ based on values for Me, n-Pr, i-Pr and n-Bu nitrites; see S. W. Benson and H. E. O'Neal, "Kinetic Data on Gas Phase Unimolecular Reactions," NBS-NSRDS-21 U.S. Department of Commerce, 1970, p. 464-469.
11. M. J. Kamlet, L. Kaplan and J. C. Dacons, *J. Org. Chem.*, 26, 4371 (1961).
12. R. Neumann, *Acct. Chem. Res.*, 5, 381 (1972).

REFERENCES (Cont.)

13. J. B. Levy, J. Am. Chem. Soc., 78, 1780 (1956).
14. The heat of formation of NO_3 is + 17 kcal/mol which together with heats of formation (kcal/mol) of HNO_3 (-32) and H^\cdot (+52) gives $D(\text{O-H})$ of 101 kcal/mol; see S. W. Benson, "Thermochemical Kinetics," John Wiley, New York, 1968, p. 199.
15. J. J. Carberry, Chem. Eng. Sci. (Genie Chimique) 9, 189 (1959).
16. D. S. Ross and N. A. Kirshen, "Industrial and Laboratory Nitrations, L. Albright and C. Hanson, ed. ACS Symposium, Ser. 22, Amer. Chem. Soc., Washington, 1976, p. 114.

Appendix B

DETONATION FAILURE DIAMETER STUDIES OF FOUR LIQUID NITROALKANES

by

C. M. Tarver, R. Shaw, and M. Cowperthwaite

DETONATION FAILURE DIAMETER STUDIES OF FOUR LIQUID
NITROALKANES*

C. M. Tarver, R. Shaw, and M. Cowperthwaite
Stanford Research Institute
Menlo Park, California 94025

Abstract: The detonation failure diameters of four liquid nitroalkanes (nitromethane, 1,1-dinitroethane, 1,1-dinitropropane, and 2,2-dinitropropane) were measured for the cases of heavy confinement in thick-walled lead cylinders and Dremm's weak shell confinement. Shock-induced reaction times and failure wave velocities in decaying detonation waves were also measured and used in the Dremm-Trofimov model to calculate failure diameters of the unconfined liquids. The Dremm-Trofimov model was found to give good agreement with experiment when the Chapman-Jouguet (CJ) properties of the steady state detonation wave are accurately known.

*This work was performed for the Office of Naval Research under Contract N000-14-70-C-0190.

Introduction

This paper presents failure diameter studies of the following nitroalkanes: nitromethane (NM), 1,1-dinitroethane (1,1-DNE), 1,1-dinitropropane (1,1-DNP), and 2,2-dinitropropane (2,2-DNP). Experiments were performed with these liquid nitroalkanes to determine their failure diameters in different types of confinement. The method developed previously for the difluoraminoalkanes¹ was used to measure the failure diameters of the liquids in thick-walled lead confinements. Shock-induced reaction times and failure wave velocities in decaying detonation waves were measured so that the semi-empirical model of Dremm-Trofimov (D-T)^{2,3} could be used to calculate failure diameters of the unconfined liquids. The experimental work is discussed first followed by the failure diameter calculations.

Problems in computing D-T failure diameters arising from uncertainties in input parameters are considered, and the methods of choosing the Chapman-Jouguet (CJ) detonation parameters for the calculations are discussed. Calculations with different values of CJ parameters show that failure diameter is extremely sensitive to the value chosen for CJ pressure in the self-sustaining detonation wave. The D-T failure diameter depends on the CJ wave parameters because it is proportional to the time required for the material to explode behind the oblique shock wave. While the explosion time depends exponentially on the pressure in the oblique shock, the shock pressure depends on the CJ pressure and the equation of state of the detonation products. The results of the calculations lead to the conclusion that the D-T model predicts realistic values of unconfined failure diameter when the failure wave velocity, the dependence of explosion time on shock pressure, and the detonation parameters in the CJ wave are known. D-T calculations based on uncertain CJ parameters

can only be expected to give failure diameters to within an order of magnitude because of the implicit exponential dependence of explosion time on CJ pressure.

Lead-Block Failure Diameters

The apparatus for determining lead-block failure diameters of liquids will not be discussed here because it has been adequately described in reference 1. A failure diameter is determined in a series of initiation experiments by decreasing the diameter of the hole containing the liquid in the lead block until the liquid fails to detonate. Experimental conditions must be chosen to ensure that detonation failure is only a result of changing the diameter of the hole. Thus, the experiments should be performed with the charge length-to-charge diameter ratio L/D greater than 3, with the initiating booster charge diameter greater than the diameter of the liquid, and with the mass of the booster greater than some minimum determined by the initiation characteristics of the liquid.

Three series of lead-block shots were performed, and the results of the first series are shown in Table 1 and in Figures 1 through 3. Nitromethane was used as a standard; its failure diameter was found to be ≤ 3.0 mm, and in good agreement with the value of 3.0 mm determined in a previous study.⁴ The failure diameters of 1,1-DNE and 1,1-DNP were found, respectively, to be 2.25 ± 0.75 mm and 11.0 ± 1.5 mm. It is interesting to note that a similar increase in failure diameter, associated with the addition of a CH_2 group, is found in the difluoraminoalkanes on going from the bisdifluoraminoalkanes to the bisdifluoramino-¹butanes.

The results of a second series of shots performed with lead blocks 50 mm in diameter and 50 mm long are shown in Table II. Experiments were performed at 60°C to determine the failure diameters of the isomers, 1,1-DNP and 2,2-DNP. Measurements on isomers are important because isomers are conceptually the most convenient compounds for studying the relationship between detonation properties and chemical structure. The 50-mm-diameter/50-mm-long lead block was found to be unsuitable for measuring the failure diameter of 2,2-DNP at 60°C, however, because liquid in a 16-mm-diameter hole failed to detonate and 16 mm represents the largest value of the diameter satisfying the condition $L/D > 3$. Consequently, a third shot was fired with 2,2-DNP at 60°C in a lead block 150 mm in diameter and 150 mm long. The liquid was contained in a 38-mm-diameter hole, and the booster was a 50-mm right cylindrical pellet of PBX 9404 (HMX). Since the liquid detonated in this configuration, the failure diameter of 2,2-DNP at 60°C was assumed to be between 16 and 38 mm and was given a value of 27 ± 11 mm because no more block shots were fired.

Shock-Induced Reaction Times

The experimental procedure for measuring shock-induced reaction times of the dinitroalkanes as a function of pressure was the same as that used previously for nitromethane and the bisdifluoraminoalkanes.^{1,5} The reaction time in a liquid shocked to a given pressure is taken as the difference between the time the shock enters the liquid and the time detonation light appears at the attenuator-liquid interface. The measured reaction times for nitromethane are shown in Figure 4 taken from reference 5. The reaction times observed for 1,1-DNE and 1,1-DNP at a preshock temperature of 25°C are shown in Figure 5, and those observed for 1,1-DNP and 2,2-DNP at a preshock temperature of 60°C are shown in Figure 6.

The length of time that the liquid remained at the initial shock pressure was computed for each experiment. This is the time required for rarefaction waves to overtake liquid at the attenuator-liquid interface and is also the lower limit for the reaction time at a pressure where detonation light is not observed. In other words, a shocked liquid exhibits detonation light when the explosion time of material at the attenuator-liquid interface is less than the time taken for rarefaction waves to overtake it and relieve the pressure. Times for rarefaction waves to quench liquid at the interface were therefore calculated to determine minimum values of the reaction times at pressures where detonation light was not observed for NM, 1,1-DNP at 25°C and 2,2-DNP at 60°C. These points are labeled "Fail" in Figures 4, 5, and 6. The calculated time was used to determine the slope of the pressure-induction time curve for 2,2-DNP at 60°C, since only two experiments were performed on this compound and detonation light was observed in one and not the other.

"Unconfined" Failure Diameters

The experiments to determine the "unconfined" failure diameters of these liquid nitroalkanes combine the features of the lead-block failure diameter shots and the smooth-shock reaction time shots. A plastic (Mylar or PVC) collar is attached to a lead block. The inside diameter of the collar is the same as the outside diameter of the lead block, namely 50.8 mm. The diameter of the hole in the lead block is larger than the lead-block failure diameter; thus, the detonation propagates through the cylinder of liquid in the hole and enters the additional liquid (12 to 25 mm deep) contained by the collar. The slit of a smear camera is focused at the top of the hole in the lead block. If the diameter of the hole is smaller than the "unconfined" failure diameter

of the liquid explosive, the detonation fails to propagate in the liquid above the hole. The smear camera film record of such a failure in nitromethane is shown in Figure 7. If the hole diameter exceeds the unconfined failure diameter, the detonation wave begins to fail when it enters the "unconfined" liquid but reinitiates before (total) failure occurs, resulting in detonation of the "unconfined" liquid. The film record of such a reinitiation in 1,1-DNE is shown in Figure 8. From these smear camera film records, the detonation velocity D_0 in the confined liquid and the failure wave velocity v in the unconfined liquid are measured. The results of these measurements are shown in Table III.

The detonation velocity of nitromethane is in good agreement with previous measurements.⁶ Dremin and Trofimov² measured a failure wave velocity of 4.75 mm/ μ sec for nitromethane, but the present measurement of 3.881 mm/ μ sec is much closer to the 3.72 mm/ μ sec measured by Davis and reported by Enig and Petrone.³ The "unconfined" failure diameter d_f of nitromethane is found to be greater than 11.76 mm. Campbell, Malin, and Holland⁷ measured failure diameters of 18 mm at 20°C and 15.7 mm at 30°C for nitromethane with weak (glass) confinement. Thus, a value of 14.3 ± 2.6 mm for NM at 25°C (the lower limit coming from Table III and the upper limit of 16.9 mm from reference 7) is used for comparison with the unconfined failure diameters calculated using the D-T model. The measured detonation and failure wave velocities, along with the measured shock-induced reaction times, are used in the D-T model calculations in the next section.

Failure Diameter Calculations

In the two-dimensional Dremin-Trofimov² (D-T) model, derived in detail by Enig and Petrone,³ a steady-state detonation wave with velocity D_0 passes from a heavy-walled tube of inner diameter $d < d_f$ (of the unconfined material) containing a liquid explosive into a region of explosive of much larger diameter than d_f . A failure wavefront quenching reaction starts at the corner and propagates at velocity v perpendicular to the direction of the self-sustaining detonation.

An oblique shock wave followed by a rarefaction fan emanates from the shrinking detonation front. If the failure wave reaches the center of the detonation wave before material behind the oblique shock front explodes, the detonation wave is extinguished. However, if the explosive in the region behind the oblique shock (region 3 in Figure 1 of reference 3) remains at the shock pressure p_3 for a time greater than the reaction induction time τ_3 corresponding to this shock pressure, reaction occurs and a new detonation wave is initiated. This wave moves through the shocked region 3 with a velocity D_3 which exceeds D_0 , overtakes the decaying original detonation front, and establishes detonation in the entire mass of liquid explosive. The unconfined failure diameter is then the diameter for which the second detonation wave reaches the center of the liquid explosive charge at the same time as the failure wave. For this type of failure the unconfined critical diameter d_f is given by the equation

$$d_f = 2u_3 v\tau_3 \left(\frac{1}{D_3 - u_3} + \frac{1}{u_3 - c_3} \right) \quad (1)$$

where u_3 and c_3 are the particle velocity and sound speed, respectively, in the stationary shock coordinate system for region 3 behind the oblique shock.

The conditions in the shocked, unreacted explosive are determined by: the geometry of the D-T model, the Chapman-Jouguet pressure p_{CJ} of the steady-state detonation wave, which is given by

$$p_{CJ} = \frac{\rho_o D_o^2}{\gamma + 1} \quad (2)$$

where ρ_o is the initial density of the liquid and γ is the adiabatic coefficient of the reaction products at the CJ state, and the Universal Hugoniot for shocked, unreacted liquids⁸ which is of the form

$$U = 1.37 c_o + 1.62 u - 0.37 c_o e^{-2u/c_o} \quad (3)$$

where U is the shock velocity, u is the particle velocity, and c_o is the sound velocity of the liquid at the initial conditions. The particle velocity u_3 in equation (1) is determined by the geometry and the Universal Hugoniot. The detonation velocity D_3 in this region is assumed to be linearly dependent on density, as originally suggested by Campbell, Davis, and Travis:⁹

$$D_3 = D_o + \left(\frac{\partial D_o}{\partial \rho_o} \right) (\rho_3 - \rho_o) = D_o + (\rho_3 - \rho_o) \left(\frac{\partial D_o}{\partial T_o} \right) \left(\frac{\partial T_o}{\partial \rho_o} \right) \quad (4)$$

where ρ_3 is the density of the liquid behind the oblique shock and T_o is the initial temperature. The $\frac{\partial D_o}{\partial \rho_o}$ term was determined from a

series of TIGER code¹⁰ calculations. Values of D_3 used in the failure diameter calculations are shown in Table IV. The sound speed c_3 is obtained from the equation

$$c_3^2 = \frac{v_3}{2} \left\{ \frac{p_3}{2} \frac{\left(\frac{dp}{dT}\right)_v}{C_v(T_3)} + \left(\frac{dp}{dv}\right)_3 \left[\frac{1}{2}(v_o - v_3) \frac{\left(\frac{dp}{dT}\right)_v}{C_v(T_3)} - 1 \right] \right\} \quad (5)$$

where

$$\left(\frac{dp}{dv}\right)_3 = -p_3 \left\{ \frac{3.24u + 1.37c_o - \left(1 - \frac{2u}{c_o}\right) (0.37c_o)e^{-2u/c_o}}{2u \left[1.62v_3 - 0.62v_o\right] - (v_o - v_3) \left[1.37c_o - \left(1 - \frac{2u}{c_o}\right) (0.37c_o)e^{-2u/c_o}\right]} \right\} \quad (6)$$

v is the specific volume. $\left(\frac{\partial p}{\partial T}\right)_v$ is a constant explained in Table V,

and $C_v(T_3)$ is the constant volume heat capacity at the shock temperature T_3 , which is determined by the Cowperthwaite-Shaw equation of state¹¹ and listed as a function of shock pressure in Table VI. The shock temperature as a function of pressure assuming a constant heat capacity is also listed in Table VI.

The remaining two terms in equation (1) are based on the experimental results. The failure wave velocity v is measured directly. The reaction induction time in region 3, τ_3 , is taken from the shock-induced reaction time curves of Figures 4, 5, and 6 using the calculated value of p_3 for each liquid. In their calculations for NM using the D-T model, Enig and Petrone³ used the theoretical reaction time τ'_3

$$\tau'_3 \approx K T_3'^2 \exp(E^\ddagger / RT_3') \quad (7)$$

where K is a constant which incorporates the Arrhenius A factor, E^\ddagger is the activation energy from low-pressure, low-temperature thermal explosion data, and T_3' is calculated from the Enig-Petrone equation of state.¹² To estimate τ_3 , Dremin and Trofimov² used the measured time difference between the passage of the failure wave and the appearance of reaction behind the oblique shock at the first point of reinitiation. This point is often quite difficult to determine from smear camera film records (see Figure 8). Therefore, the shock-induced reaction curves of Figures 4, 5, and 6 are used to determine τ_3 , once p_3 is determined.

The shock pressure p_3 behind the oblique shock front depends on the relationship between v and D_o , which determines the geometry, and the CJ pressure. Thus, accurate values of p_{CJ} are essential for the failure diameter calculations. Of the four liquid nitroalkanes used, the CJ pressure is well-known only for NM. The widely accepted value of p_{CJ} for NM is 127 kbar.¹³ Kamlet¹⁴ has developed an empirical equation relating the adiabatic exponent γ to ρ_o :

$$\gamma = \frac{0.656}{\rho_o} + 0.703 + 1.105 \rho_o \quad (8)$$

Replacing γ in equation (2) by equation (8) yields p_{CJ} in terms of ρ_o and D_o :

$$p_{CJ} = \rho_o^2 D_o^2 / \left(1.105 \rho_o^2 + 1.703 \rho_o + 0.656 \right) \quad (9)$$

Equation (9) for p_{CJ} gives 126.1 kbar for NM with the measured values: $\rho_o = 1.127 \text{ g/cm}^3$ and $D_o = 6.285 \text{ mm}/\mu\text{sec}$.

Table VII shows a comparison between the experimentally measured unconfined failure diameters and those calculated using equation (9) for p_{CJ} . The calculated and observed values of d_f for NM and 1,1-DNE agree quite well, but the calculated values of d_f of 1,1-DNP and 2,2-DNP are at least a power of ten larger than the experimental values. The reaction times τ_3 are a power of ten longer for the DNPs than for NM and 1,1-DNE, indicating that the oblique shock pressures p_3 and hence the CJ pressures (p_{CJ}) predicted by equation (9) for the DNPs are too low. In the case of 1,1-DNP at 60°C, it has already been mentioned that D_o was not measurable from the film records. However, enough data exist for the isomers 1,1-DNP and 2,2-DNP that the inverse method, developed by Wood and Fickett¹⁵ and used successfully for NM and Acenina by Davis,¹⁶ can be used to calculate p_{CJ} for 1,1-DNP at 60°C. Table VIII contains inverse method calculations of p_{CJ} and failure diameter d_f for various values of D_o for 1,1-DNP at 60°C. The minimum calculated failure diameter for 1,1-DNP at 60°C is obtained for $p_{CJ} = 138.1$ kbar [5.5 kbar higher than the value of p_{CJ} which corresponds to the value of γ calculated in equation (8)]. However, this calculated value of d_f is still a power of ten larger than the experimental value of d_f for 1,1-DNP at 60°C. The calculations for 1,1-DNP are also complicated by the fact that the quantity $u_3 - c_3$ is much smaller for 1,1-DNP than for the other three liquids and hence affects d_f much more strongly. As shown in Table VIII, this quantity may even be negative, which clearly is physically impossible. The explanation for this situation is not available at present.

The minimum calculated failure diameter for 1,1-DNP at 60°C in Table VIII was obtained using a larger p_{CJ} than the one predicted by equation (9), which is based on an empirical fit to NM data. This correlation can be qualitatively explained by considering the oxygen balance of the

explosives and hence the relative amounts of reaction products produced. Table IX contains TIGER code¹⁰ calculations of the reaction products at the CJ state using the Kistiakowsky-Wilson equation of state¹⁷ for the four nitroalkanes. NM and 1,1-DNE produce similar quantities of most reaction products since their oxygen balances are roughly equal, while the DNPs, which have a poorer oxygen balance, produce more than three times as much solid carbon as NM and 1,1-DNE. Zeldovich and Kompanets¹⁸ show that the adiabatic coefficient γ of the reaction products decreases as the amount of solid carbon increases, thereby increasing the relative value of p_{CJ} in equation (2).

An additional set of failure diameter calculations for 1,1-DNP at 25°C and 2,2-DNP at 60°C was made using larger values for p_{CJ} . These calculations are shown in Table X, along with the best results for NM and 1,1-DNE (from Table VII) and 1,1-DNP at 60°C (from Table IX). The value of p_{CJ} used for 1,1-DNP at 25°C is based on the change in p_{CJ} with initial temperature from TIGER calculations¹⁰ and the value of 138.1 kbar used for 1,1-DNP at 60°C. The value of p_{CJ} used for 2,2-DNP is based on the difference in p_{CJ} between 1,1-DNP and 2,2-DNP predicted by TIGER calculations.¹⁰ The agreement between the calculated and observed failure diameters for these two cases has been improved considerably by this arbitrary increase in p_{CJ} . Table X demonstrates the importance of an accurate knowledge of p_{CJ} .

Discussion of Results and Conclusions

The results of the failure diameter calculations show that the D-T model yields excellent agreement with observed "unconfined" failure diameters when the CJ pressure, independently measured shock-induced reaction times, and failure wave velocities are accurately known. Because of the large volume of data on p_{CJ} and shock-induced reaction times

(Figure 4) for NM, its unconfined failure diameter is well determined in the D-T model. However, the use of fragmentary data on any of the important parameters (p_{CJ} , v , or τ_3) can cause the D-T model predictions to be wrong by a power of ten, as shown in Table X for 1,1-DNP at 60°C. Since the required experimental data are attainable in a relatively simple geometry and are directly related to a failure mechanism, the D-T model represents an improvement over other unconfined failure diameter theories¹⁹⁻²² which are based on the curvature of the detonation wave in confined and unconfined explosive charges.

The experimental problem of obtaining a reliable value of p_{CJ} represents one of the limiting factors in the use of the D-T model. Davis and Venable²³ compared five techniques to measure p_{CJ} for Composition B-3 and found that the results vary by approximately 16%. Comparing the d_f calculations for 2,2-DNP in Tables VII and X, a 12% change in p_{CJ} resulted in a factor of 7 change in d_f . Since the shock pressure-reaction time curves largely determine the variation in d_f and the shock pressure p_3 depends on p_{CJ} , reliable values of p_{CJ} are essential for unconfined failure diameter calculations in the D-T model.

While shock-induced reaction times and failure wave velocities can be accurately measured, their relationships to chemical kinetics are not completely understood. The shock-induced reaction time as a function of shock pressure cannot be expressed in an equilibrium Arrhenius form, such as equation (7), because of the uncertainty in shock temperature as a function of pressure.^{11,12} Two chemical structure effects, the methylene effect and the α -hydrogen effect, are apparent in Figures 5 and 6. The methylene effect is shown in Figure 5, since 1,1-DNE requires a lower shock pressure (~ 10 kbar lower) to react in a certain length of time than the next member of the homologous series, 1,1-DNP, which differs only by a $-\text{CH}_2-$ group. The α -hydrogen effect is observed in Figure 6

when two compounds of similar structure are compared, one (1,1-DNP) which has a hydrogen atom α to the dinitrocarbon atom and one (2,2-DNP) which does not. The compound without the α -hydrogen (2,2-DNP) exhibits a much higher shock pressure for a certain reaction time than the compound with the α -hydrogen (1,1-DNP). The decrease in reaction time at a particular shock pressure as the initial temperature increases is observed by comparing 1,1-DNP at $T_0 = 25^\circ\text{C}$ in Figure 5 and $T_0 = 60^\circ\text{C}$ in Figure 6. Additional work is necessary to quantify these observed effects.

The measured failure wave velocities exhibit a dependence on the shock-induced reaction times. The failure wave velocities relative to the detonation velocities increase as the shock pressures required for reaction at a specified time increase. The rate of detonation failure is related to the shock sensitivity of the liquid in region 3 behind the oblique shock wave of the D-T model in a complex manner. This relationship probably involves the CJ sound velocity, transverse wave velocity, and cell spacing in the three-dimensional microstructure of self-sustaining detonation waves. This cellular microstructure is well-known for gas phase detonations²⁴ and has been observed in detonations of nitromethane diluted with acetone.²⁵ Additional theoretical and experimental research is required to determine the nature of these failure waves.

Acknowledgments

We gratefully acknowledge G. S. Cartwright, A. Urweider, C. M. Benson, E. Daigle, and L. B. Hall, who did most of the experimental work, and R. W. Woolfolk who helped analyze the results. We also thank Stanford Research Institute for support during the preparation of this paper.

References

1. L. B. Seely, J. G. Berke, R. Shaw, D. Tegg, and M. W. Evans, "Failure Diameter, Sensitivity, and Wave Structure in Some Bis-difluoramino alkanes," Proceedings of Fifth Symposium (International) on Detonation, Pasadena, 1970, ACR-184, Office of Naval Research, Department of the Navy, Arlington, Virginia, p. 89.
2. A. N. Dremin and V. S. Trofimov, "On the Nature of the Critical Diameter," Tenth Symposium (International) on Combustion, The Combustion Institute, 1965, p. 829.
3. J. W. Enig and F. J. Petrone, "The Failure Diameter Theory of Dremin," Proceedings of Fifth Symposium (International) on Detonation, Pasadena, 1970, ACR-184, Office of Naval Research, Department of the Navy, Arlington, Virginia, p. 99.
4. L. B. Seely, unpublished data.
5. R. Shaw, Combust. Flame 21, 127 (1973).
6. B. M. Dobratz, Properties of Chemical Explosives and Explosive Simulants, UCRL-51319 Rev. 1, July 31, 1974.
7. A. W. Campbell, M. E. Malin, and T. E. Holland, J. Appl. Phys. 27, 963 (1956).
8. R. W. Woolfolk, M. Cowperthwaite, and R. Shaw, Thermochem. Acta 5, 409 (1973).
9. A. W. Campbell, W. C. Davis, and J. R. Travis, Phys. Fluids 4, 498 (1961).
10. M. Cowperthwaite and W. H. Zwisler, Improvement and Modification to TIGER Code, Final Report under Contract N60921-72-C-0013, January 1973.
11. M. Cowperthwaite and R. Shaw, J. Chem. Phys. 53, 555 (1970).
12. J. W. Enig and F. J. Petrone, Phys. Fluids 9, 398 (1966).
13. F. J. Petrone, Phys. Fluids 11, 1473 (1968).
14. M. J. Kamlet, private communication.
15. W. W. Wood and W. Fickett, Phys. Fluids 6, 648 (1963).
16. W. C. Davis, Proceedings of the Fifth Symposium (International) on Detonation, Pasadena, 1970, ACR-184, Office of Naval Research, Department of the Navy, Arlington, Virginia, p. 75 (Discussion of paper by W. H. Andersen, et al.).

17. R. D. Cowan and W. Fickett, J. Chem. Phys. 24, 932 (1956).
18. Ya. B. Zeldovich and A. S. Kompaneets, Theory of Detonation, (Academic Press, New York, 1960), Chapter Four.
19. H. Eyring, R. E. Powell, G. H. Duffey, and R. B. Parlin, Chem. Revs. 45, 69 (1949).
20. H. Jones, Proc. Roy. Soc. (London) A189, 415 (1947).
21. W. W. Wood and J. G. Kirkwood, J. Chem. Phys. 22, 1920 (1954).
22. M. W. Evans, J. Chem. Phys. 36, 193 (1962).
23. W. C. Davis and D. Venable, "Pressure Measurements for Composition B-3," Proceedings of the Fifth Symposium (International) on Detonation, Pasadena, 1970, ACR-184, Office of Naval Research, Department of the Navy, Arlington, Virginia, p. 13.
24. R. A. Strehlow, Combust. Flame 12, 81 (1968).
25. P. A. Urtiew, A. S. Kusubov, and R. E. Duff, Combust. Flame 14, 117 (1970).

Table I. First series of lead-block failure diameter measurements on liquid dinitroalkanes at 25° C. ^a

Compound	Charge		Charge Weight/ L/D	Charge Weight/ g	Transit Time/ μsec	Detonation Velocity/ (mm/μsec)	RDX Pellet		RDX Pellet Weight/ g	Failure Diameter/ mm
	Length/ mm	Diameter/ mm					Diameter/ mm	Length/ mm		
NM	49.4	12.5	4.0	5.5	7.6	6.5	19	19	8.65	≤ 3
See Fig. 1	50.4	4.5	11.2	0.6	7.9	6.3	12.7	6.4	1.29	
	49.6	3.0	16.5	0.3	7.9	6.3	12.7	6.4	1.29	
1,1-DNE	50.8	4.5	11.2	0.8	7.0	7.3	12.7	6.4	1.29	2.25±0.75
See Fig. 2	50.4	3.0	16.8	0.4	7.0	7.3	12.7	6.4	1.29	
	50.8	1.5	33.9	0.1	∞	0	12.7	6.4	1.29	
	18.9	1.5	12.6	0.03	∞	0	12.7	6.4	1.29	
1,1-DNP	305	12.5	24.4	45	50.0	6.1	19	19	8.65	
See Fig. 3	51.0	12.5	4.1	7.5	7.9	6.5	19	19	8.65	
	49.4	12.5	4.0	7.5	7.8	6.3	19	19	8.65	
	49.4	12.5	4.0	7.5	7.8	6.3	19	19	8.65	
	50.7	12.5	4.1	7.5	7.6	6.7	19	6.4	2.95	11.0±1.5
	50.7	11.0	4.6	5.6	∞	0	19	19	8.65	
	50.2	11.0	4.6	5.6	7.8	6.4	19	6.4	2.95	
	50.7	11.0	4.6	5.6	∞	0	19	6.4	2.95	
	50.8	11.0	4.6	5.6	∞	0	19	6.4	1.29	
	50.8	9.5	5.4	4.4	∞	0	12.7	6.4	1.29	
	50.7	9.5	5.4	4.4	∞	0	12.7	6.4	1.29	
	50.7	8.0	6.3	2.5	∞	0	12.7	6.4	1.29	
	50.6	8.0	6.3	2.5	∞	0	12.7	6.4	1.29	
	53.6	7.5	7.2	2.2	∞	0	12.7	6.4	1.29	
	50.2	3.0	16.7	0.3	∞	0	12.7	6.4	1.29	

^a In all experiments the outside diameter of the lead block was 50 mm.

Table II. Second series of lead-block failure diameter measurements on liquid dinitroalkanes.^a

Compound	Temperature/ °C	Charge Diameter/ mm	Charge L/D	Transit Time/ μsec	Detonation Velocity/ (mm/μsec)	Failure Diameter/ mm
1,1-DNP	60	8.0	6.3	8.4	6.0	} 7 ± 1
	60	6.0	8.4	∞	0	
2,2-DNP	60	12.5	4.0	∞	0	} > 16
	60	12.5	4.0	∞	0	
	60	16.0	3.1	∞	0	
	60	16.0	3.1	∞	0	

^aIn all experiments the outside diameter of the lead block was 50 mm, the charge length was 50 mm, and the Detasheet (PETN) pellet was 19 mm long, 19 mm in diameter, and weighed 8.0 g.

Table III. Experimental results.

Compound	T ₀ (°C)	Lead Block Diameter (mm)	D ₀ ($\frac{\text{mm}}{\mu\text{sec}}$)	v ($\frac{\text{mm}}{\mu\text{sec}}$)	Average D ₀ ($\frac{\text{mm}}{\mu\text{sec}}$)	Average v ($\frac{\text{mm}}{\mu\text{sec}}$)	Unconfined Failure Diameter d _f (mm)
NM	25	11.76	6.266	3.894	6.285 ± 0.018	3.881 ± 0.013	> 11.76
NM	25	11.76	6.303	3.868			
1,1-DNE	25	4.521	6.925	2.353	6.938 ± 0.013	2.200 ± 0.153	2.39 ± 0.79 ^a
1,1-DNE	25	3.175	6.951	2.047			
1,1-DNP	25	15.85	6.431	3.088	6.414 ± 0.018	3.110 ± 0.021	> 15.85
1,1-DNP	25	15.85	6.396	3.131			
1,1-DNP	60	12.50	b	2.966	b	2.966	< 12.50
2,2-DNP	60	38.35	6.318	5.022	6.318	5.022	> 38.35 ^c

^a Reinitiation occurred at 3.175 mm diameter and failure at 1.60 mm.

^b The detonation velocity could not be determined.

^c Very close to actual failure diameter since several reaction sites (none strong enough to reinitiate detonation) were observed.

Table IV. Calculation of D_3 .

Compound	Initial Temperature ($^{\circ}$ C)	D_0 (mm/ μ sec)	$(\partial D_0 / \partial \rho_0)$ (mm-cc/ μ sec-g)	$(\rho_3 - \rho_0)$ (g/cc)	D_3 (mm/ μ sec)
NM	25	6.285	3.244	0.703	8.566
1,1-DNE	25	6.938	2.879	0.821	9.302
1,1-DNP	25	6.414	3.327	0.755	8.926
1,1-DNP	60	6.274 ^a	3.327	0.728	8.696
2,2-DNP	60	6.318	3.327 ^b	0.818	9.039

(from TIGER)

^aThe detonation velocity for 1,1-DNP at 60 $^{\circ}$ C was not measured. This value of D_0 yields the best failure diameter calculation and is consistent with $\partial D_0 / \partial \rho_0$ from TIGER calculations.

^bSince only one initial temperature was calculated in TIGER, 2,2-DNP is assumed to have the same $\partial D_0 / \partial \rho_0$ as 1,1-DNP.

Table V. Input data for c_3 and u_3 .

Quantity	Units	NM	1,1-DNE ^a	1,1-DNP ^a	2,2-DNP ^a
$(\partial p / \partial T)_v^b$	$10^7 \text{ dyn cm}^{-2} \text{ deg}^{-1}$	1.63	1.58	1.65	1.65
Sound speed					
at 25°C	10^5 cm sec^{-1}	1.30	1.27	1.39	---
at 60°C	---	---	---	1.33	1.24
Specific volume					
at p = 0					
at 25°C	cc g^{-1}	0.884	0.738	0.797	---
at 60°C	---	---	---	0.833	0.819
Molecular wt	g mol^{-1}	61.0	120.1	134.1	134.1
C_v (constant) ^c					
at 25°C	$\text{cal mol}^{-1} \text{ deg}^{-1}$	17.8	37.9	43.4	---
at 60°C	---	---	---	---	46.1
C_v fit ^d					
$10^{-6} B$	---	1.23375	3.044	---	3.502
$10^{-4} C$	---	-0.995686	-2.506	---	-2.964
$10^{-1} D$	---	1.73573	5.092	---	6.027
$10^3 E$	---	8.09421	-3.368	---	-0.4161
$10^6 F$	---	-2.24624	0.8369	---	0.1459

^aThe physical properties v_0 , α , C_p , C_v , and c_0 were measured.

^bCalculated from $(\partial p / \partial T)_v = \alpha C_v c_0^2 / V_0 C_p$ where α is the coefficient of expansion c_0 is the sound speed, V_0 is the specific volume at p = 0, C_v is the heat capacity at constant volume, and C_p is the heat capacity at constant pressure.

^c C_v was calculated from $C_v = C_p / \{1 + [(M \alpha^2 c_0^2) (2.39 \times 10^{-8}) / C_p]\}$ where M is the molecular weight and 2.39×10^{-8} corrects the units.

^d $C_v(T)$ is given by $C_v [\text{constant} + (B/T^2) + (C/T) + D + (E \times T) + (F \times T^2)]$.

Table VI. Calculated shock temperatures.

Liquid	Equation of State	Preshock Temp (°K)	Shock Temperature (°K)	25	50	75	100	125	150	175	200
NM	CSUBV	298	513	746	1022	1319	1643	2097	2958	4740	
NM	CSUBV (T)	298	484	646	810	979	1149	1316	1483	1669	
1,1-DNE	CSUBV	298	447	612	807	1025	1256	1499	1777	2150	
1,1-DNE	CSUBV (T)	298	447	587	732	883	1037	1192	1346	1504	
1,1-DNP	CSUBV	298	451	619	820	1043	1279	1533	1842	2297	
1,1-DNP	CSUBV (T)	298	433	559	689	824	961	1099	1236	1375	
1,1-DNP	CSUBV	333	504	681	890	1121	1362	1633	2018	2696	
1,1-DNP	CSUBV (T)	333	477	605	738	877	1020	1161	1302	1450	
2,2-DNP	CSUBV	333	512	694	909	1145	1389	1667	2072	2804	
2,2-DNP	CSUBV (T)	333	483	614	749	891	1035	1179	1321	1470	

Table VII. Comparison of measured failure diameters with those calculated using experimental data where possible, CJ pressures calculated using Kamlet's equation, and the C(T) method of calculating shock temperature.

Com- pound	Initial Temp (°C)	ρ_0 (g/cc)	D_0 (mm/ μ sec)	v (mm/ μ sec)	γ	P_{CJ} (kbar)	P_3 (kbar)	T_3 (μ sec)	C in		d_f (mm)	
									$d_f = cT^3$	$d_f = cT^3$	calc.	exptl.
NI	25	1.127	6.285	3.881	2.530	126.1	93.0	0.138	102	14.1	16.85	
1,1-DNT	25	1.355	6.938	2.200	2.684	177.1	98.4	0.0657	41.0	2.69	2.39 \pm 0.79	
1,1-DNP	25	1.254	6.414	3.110	2.612	142.8	97.7	1.59	106	169	>15.85	
1,1-DNP	60	1.201	6.283 ^a	2.966	2.576 ^a	132.6 ^a	89.8	2.65	103	273	9.25 \pm 3.25	
2,2-DNP	60	1.221	6.318	5.022	2.589	135.8	104.9	3.96	97.1	383	>38.35	

^a Since D_0 was not measured, P_{CJ} and D_0 for this value of γ were obtained by the inverse method (see Table VIII).

Table VIII. Inverse method calculations of P_{CJ} and d_f for 1,1-DNP at $T_0 = 60^\circ C$

D_0 ($\frac{mm}{\mu sec}$)	P_{CJ} (kbar)	γ	P_3 (kbar)	D_3^{-u}	u_3^{-c}	c in $d_f = c\tau_3$	τ_3 (μsec)	d_f (calc) (mm)	d_f (obs) (mm)
6.263	146.5	2.216	105.35	2.952	-0.192	-168.1	0.0400	-6.724	9.25 ± 3.25^a
6.268	142.4	2.315	101.10	2.869	-0.032	-1076	0.9394	-101.1	a
6.270	140.8	2.352	98.88	2.825	0.050	711.8	0.2228	158.6	
6.272	139.5	2.387	97.58	2.797	0.103	353.2	0.3114	110.0	
6.273	138.6	2.411	96.58	2.777	0.142	260.2	0.4304	112.0	
6.274	138.1	2.422	96.00	2.764	0.169	221.0	0.4788	105.8	b
6.275	137.3	2.445	95.05	2.745	0.199	190.1	0.6556	124.6	
6.279	134.9	2.511	92.39	2.694	0.296	132.9	1.332	177.0	
6.283	132.6	2.576 ^c	89.80	2.640	0.397	103.3	2.650	273.7	

^a Negative values of c and d_f obtained.

^b Minimum value of d_f obtained.

^c Matches γ in Kamlet's equation (8).

Table IX. Reaction products calculated by the TIGER code
(moles of product per mole of explosive)

Product Gases	NM ^a (T _o = 25° C)	1,1-DNE (T _o = 25° C)	1,1-DNP (T _o = 25° C)	1,1-DNP (T _o = 60° C)	2,2-DNP (T _o = 60° C)
H ₂ O	2.198	1.532	2.237	2.190	2.225
N ₂	0.9632	0.9787	0.9659	0.9636	0.9647
CO ₂	0.7379	1.074	0.7641	0.7487	0.7518
CO	0.3266	0.3203	0.2348	0.3123	0.2720
CH ₄	0.1335	0.05311	0.1055	0.1273	0.1175
NH ₃	0.07365	0.04303	0.06819	0.07275	0.07070
H ₂	0.01508	0.00506	0.00854	0.01341	0.01109
C ₂ H ₆	0.1138	0.00776	0.1207	0.1193	0.1168
C ₃ H ₈	0.01692	0.01484	0.01970	0.01859	0.01820
C ₃ H ₆	0.0009	0.00004	0.00005	0.00008	0.00007
CH ₃	0.00006	0.00006	0.00003	0.00005	0.00004
NO	0.00002	0.00008	0.00001	0.00003	0.00003
Total gas	4.579	4.099	4.525	4.566	4.547
C (solid)	0.5235	0.3532	1.596	1.517	1.570

^aFor ease of comparison, the number of moles of product per two moles of nitromethane is listed.

Table X. Best failure diameter calculations

Compound and Method Used	ρ_0 (g/cc)	D_0 (mm/μsec)	v (mm/μsec)	γ	P_{CJ} (kbar)	P_3 (kbar)	T_3 (μsec)	c in $d_f = cT_3$	d_f (calc.) (mm)	d_f (exp't.) (mm)
Nitromethane $T_0 = 25^\circ C$ [Kamlet's Eq. (8)]	1.127	6.285	3.881	2.530	126.1	93.00	0.1377	102.00	14.05	16.85
1,1-DME $T_0 = 25^\circ C$ [Kamlet's Eq. (8)]	1.355	6.938	2.200	2.684	177.1	98.41	0.06570	41.00	2.694	2.39±0.79
1,1-DMP $T_0 = 25^\circ C$ [Inverse and by CJ TIGER]	1.254	6.414	3.110	2.401	151.7	107.2	0.1000	391.2	39.12	>15.85
1,1-DMP $T_0 = 60^\circ$ (Inverse Method)	1.201	6.274	2.966	2.422	138.1	96.00	0.4788	221.0	105.8	9.25±3.25
2,2-DMP $T_0 = 60^\circ$ (by CJ TIGER)	1.221	6.318	5.022	2.194	152.6	124.7	0.3784	148.1	56.04	≥38.35

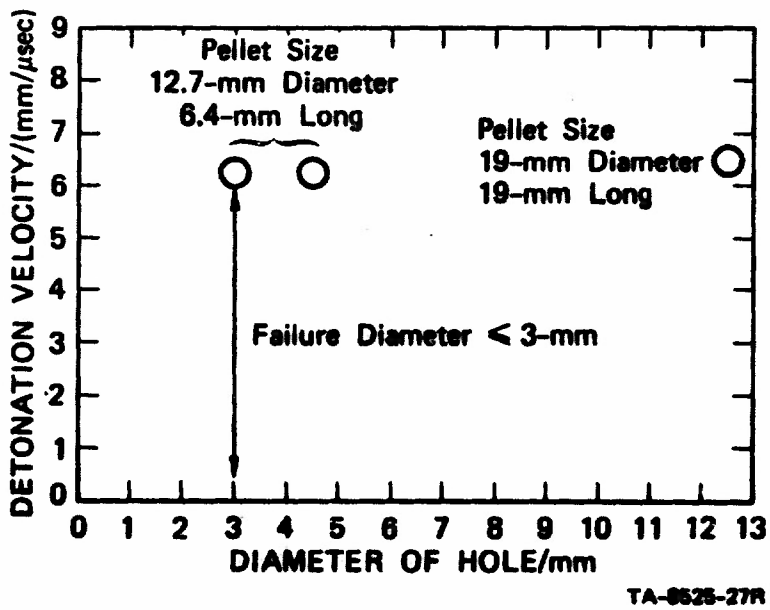
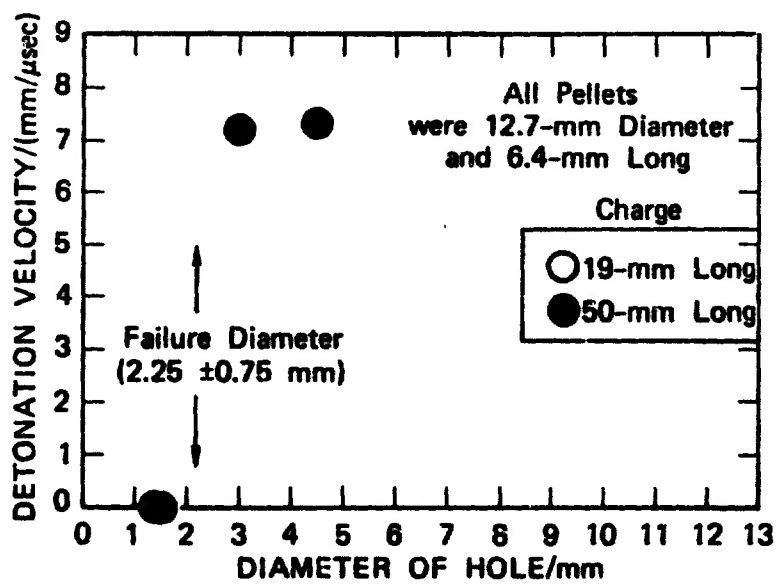


FIGURE 1 LEAD-BLOCK FAILURE DIAMETER OF NITROMETHANE



TA-8525-28R

FIGURE 2 LEAD-BLOCK FAILURE DIAMETER OF 1,1-DNE

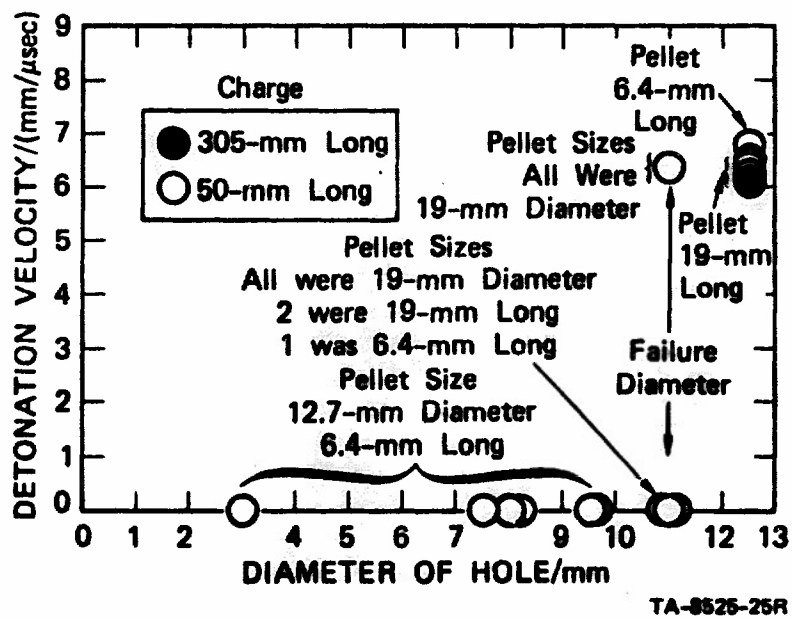
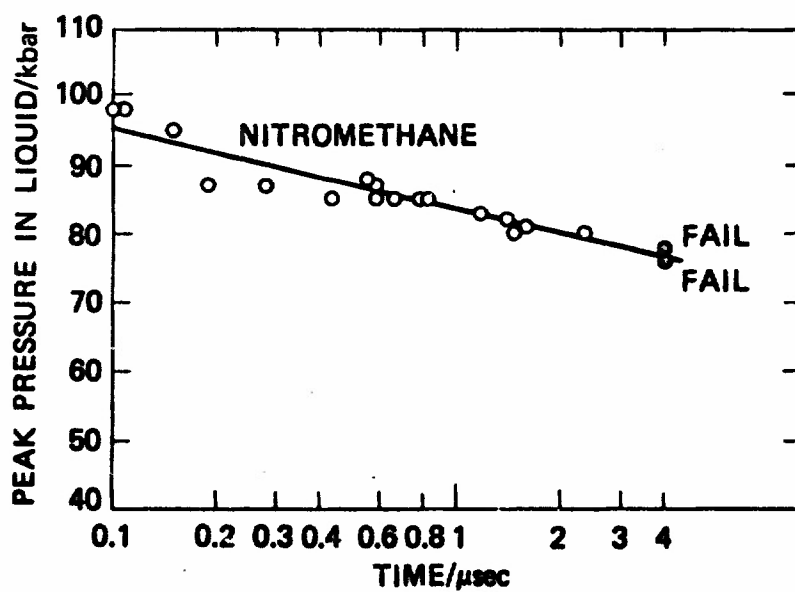
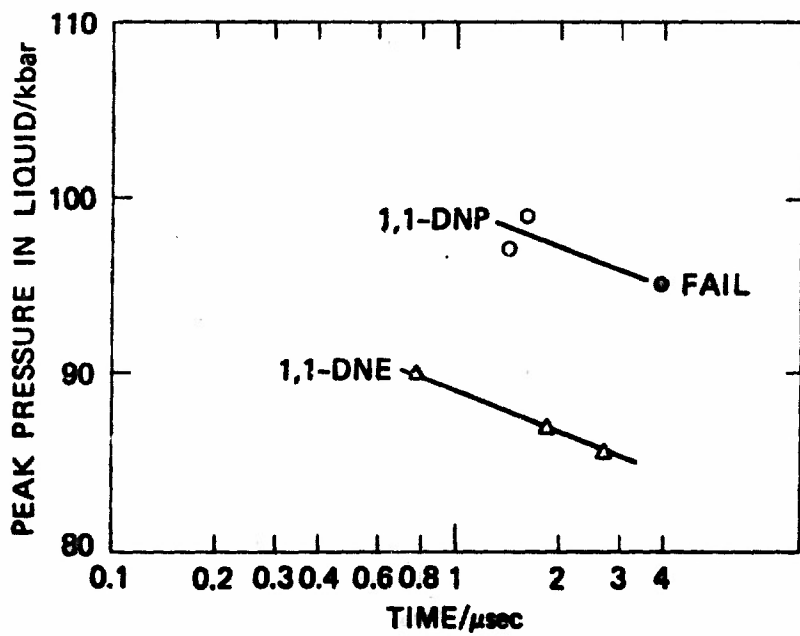


FIGURE 3 LEAD-BLOCK FAILURE DIAMETER OF 1,1-DNP



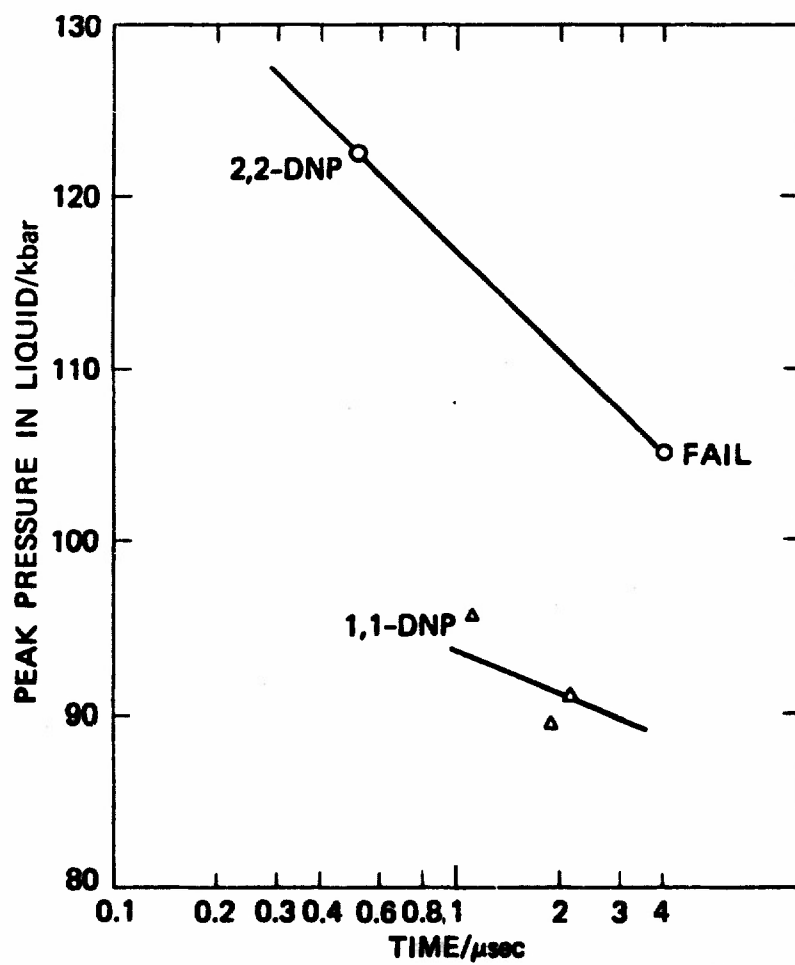
TA-8525-51R

FIGURE 4 SMOOTH-SHOCK REACTION TIME MEASUREMENTS FOR NITROMETHANE AT A PRESHOCK TEMPERATURE OF 25°C



TA-8525-56R

FIGURE 5 SMOOTH-SHOCK REACTION TIME MEASUREMENTS FOR 1,1-DNE AND 1,1-DNP AT A PRESHOCK TEMPERATURE OF 25°C



TA-8525-57R

FIGURE 6 SMOOTH-SHOCK REACTION TIME MEASUREMENTS FOR 1,1-DNP AND 2,2-DNP AT A PRESOCK TEMPERATURE OF 60°C

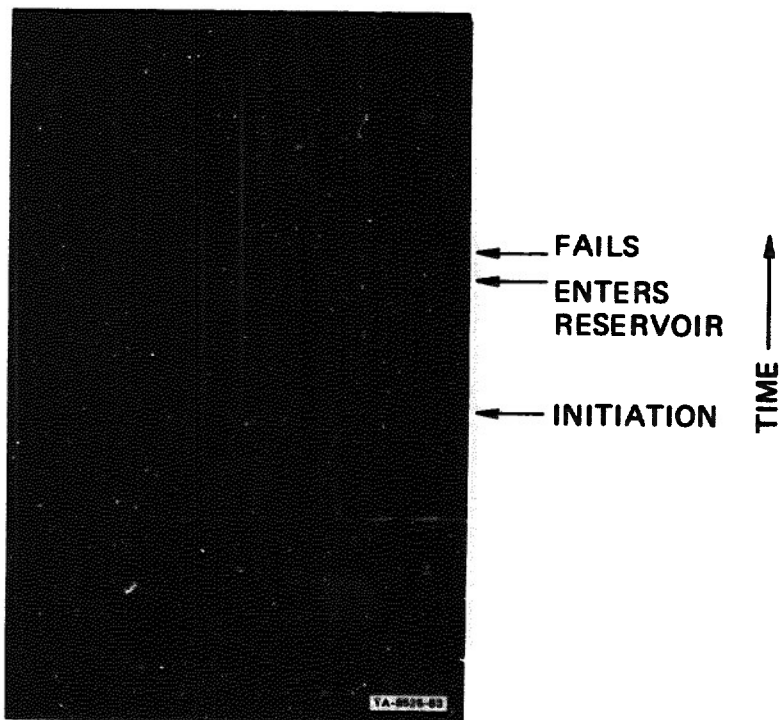


FIGURE 7 SMEAR CAMERA FILM RECORD OF A
DETONATION IN NITROMETHANE
TRAVELING IN A 11.76 mm DIAMETER HOLE,
50 mm LONG, IN A 50 mm DIAMETER LEAD
BLOCK AND ENTERING A 50 mm DIAMETER
RESERVOIR OF NITROMETHANE

Time scale on photograph 0.25 $\mu\text{sec}/\text{mm}$.

FIGURE 8 SMEAR CAMERA FILM RECORD OF A
DETONATION IN 1,1-DNE TRAVELING IN A
4.5 mm DIAMETER HOLE, 50 mm LONG, IN A
50 mm DIAMETER LEAD BLOCK AND
ENTERING A 50 mm DIAMETER RESERVOIR
OF 1,1-DNE

Time scale on photograph $0.25 \mu\text{sec}/\text{mm}$.

B-34

Appendix C

THE VERY LOW-PRESSURE PYROLYSIS OF DINITROPROPANES

by

David S. Ross and Leonard W. Piskiewicz

THE VERY LOW-PRESSURE PYROLYSIS
OF DINITROPROPANES

by

David S. Ross* and Leonard W. Piszkiwicz

Abstract

The unimolecular decomposition of four dinitropropanes has been studied using the recently developed very low-pressure pyrolysis (VLPP) technique. 1,2-Dinitropropane was found to undergo cyclic elimination of HONO, similar to the unimolecular decomposition of simple mononitroalkanes. The products were 1- and 2-nitropropene, and the rate constant for the process was $\log k/(\text{sec}^{-1}) = 11.3 - 40/\theta$. The three gem-dinitroalkanes, 1,1- and 2,2-dinitropropane and 1-fluoro-1,1-dinitropropane underwent C-N scission rather than HONO elimination due to a weakening of the C-N bonds, the result of α -nitro substitution. The three compounds decomposed with essentially the identical rate constant, $\log k/(\text{sec}^{-1}) = 17.0 - (47 \pm 1)/\theta$. Major decomposition products in these cases were carbonyl compounds, propionaldehyde, and acetone in the case of the 1,1- and 2,2-dinitropropanes, and propionyl fluoride in the case of 1-fluoro-1,1-dinitropropane. These products can be explained by a mechanism involving initial C-N scission, followed by intramolecular oxygen transfer from nitrogen to carbon in the resulting nitropropyl radical.

Introduction

Several investigations of the gas-phase thermal decomposition of mono-nitroalkanes have been reported over the past two decades, and the results have shown that generally the compounds undergo a cyclic elimination of HONO with an activation energy in the range 43 ± 3 kcal/mole.^{1,2} Arrhenius A-factors have ranged $10^{11} - 10^{13}$ sec⁻¹ and, while a value of about $10^{11.3}$ sec⁻¹ appears to be the favored experimental parameter, for theoretical reasons a value of about $10^{13.5}$ sec⁻¹ is preferred.² Thus, while the "tightness" of the transition state is in question, its cyclic nature is clear.

The gas-phase thermal decomposition of gem-polynitroalkanes has been less well studied. There are some accounts of studies in this area,^{3a-f} and on the basis of the kinetic parameters obtained (Table 1) it was suggested that the compounds undergo C-N scission rather than cyclic elimination.^{3d} The change in mechanism was explained in terms of a weakened C-N bond due to α -NO₂ substitution.

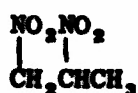
While such a mode of decomposition is reasonably likely in the methane cases, the likelihood of complicating radical chain processes in the ethanes and propanes exists. This possibility is a particularly important consideration in view of the fact that the pressures used in the studies were in the range 30-200 torr, and, moreover, only limited product data were obtained.⁴

In order to bring about a detailed understanding of the decomposition of polynitroalkanes, we have carried out a study of the unimolecular decomposition of four dinitropropanes with sufficiently different structures to provide a means of distinguishing between the possible modes of decomposition.



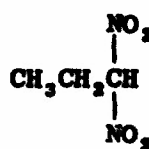
2,2-dinitropropane

2,2-DNP



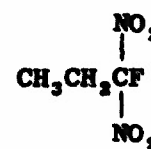
1,2-dinitropropane

1,2-DNP



1,1-dinitropropane

1,1-DNP



1-fluoro-1,1-dinitropropane

1,1,1-FDNP

Table I
KINETIC PARAMETERS FOR THE GAS-PHASE UNIMOLECULAR
DECOMPOSITION OF POLYNITROALKANES

Compound	log A (A/sec ⁻¹)	E _a (kcal/mole)	Reference
<u>Methanes</u>			
IC(NO ₂) ₃	15.3	34	3(f)
BrC(NO ₂) ₃	16.1	36	3(f)
ClC(NO ₂) ₃	15.8	36	3(f)
FC(NO ₂) ₃	15.4	42	3(e)
Cl ₂ C(NO ₂) ₂	15.3	34	3(c)
F ₂ C(NO ₂) ₂	15.9	47	3(e)
CH ₃ NO ₂	15.6	59	2
<u>Ethanes and Propanes</u>			
C(NO ₂) ₄	16.3	38	3(e)
	17.5	41	3(a)
CH ₃ C(NO ₂) ₃	17.2	43	3(c)
CH ₃ CH ₂ C(NO ₂) ₃	16.9	42	3(c)
CH ₃ HC(NO ₂) ₂	16.7	47	3(d)
CH ₃ FC(NO ₂) ₂	17.0	48	3(e)
CH ₃ CH ₂ HC(NO ₂) ₂	16.9	48	3(d)
(CH ₃) ₂ C(NO ₂) ₂	18.5	51	3(b)

The study was made using the very low-pressure pyrolysis (VLPP) technique developed and exploited by Benson et al.^{5a-1} The method essentially eliminates wall catalyzed and radical chain reactions, and in our version allows the collection and identification of reaction products.

Experimental

Materials--The nitro compounds were made by published methods.⁶

VLPP Apparatus--The reactor is a cylindrical quartz vessel, 6.5 cm long and 5.0 cm in diameter, heated with a clam shell heater. The pressure within the system is typically 10^{-4} - 10^{-3} torr. The material to be studied enters the reactor at one end through an inlet tube leading from a variable needle valve, and the fragments emerge through the exit orifice in the reactor base. A quadrupole mass spectrometer head is positioned immediately below the orifice.

The reactor can be operated at three different collision numbers. This objective is attained through an assembly in which a cutaway quartz disc with two holes and a polished bottom surface rests on the polished upper surface of the base of the reactor. The disc can be rotated by means of a rod passing from an external control knob through the center of the reactor. An aperture through the reactor base 10.3 mm in diameter is located off center, such that the upper plate can be positioned to expose the base hole through the cutaway portion of the plate. This alignment provides a collision number of 176.

Alternatively, the plate can be rotated such that one of its holes is positioned over the base hole, reducing the area of the exit aperture of the reactor, and increasing the collision number of the system. A 3.1-mm plate aperture provides a collision number of 1930, and an 0.81-mm aperture, 29,000 collisions. This multicollision number arrangement allows measurement of reaction rates of more than four orders of magnitude.

The materials were stored as liquids (solid in the case of 2,2-DNP) in a small sample volume above the needle valve. During a run the samples were heated to provide a vapor pressure of several torr. In this way an effective reservoir of sample vapor could be maintained for a number of hours of experimental time.

Kinetic Runs--The mass spectra of the compounds under study show no parent peak, even at low ionization potentials. In each case a prominent peak characteristic of the starting material, established by observing the mass spectrum of the material with the reactor at room temperature, was monitored with increasing reactor temperature. This base peak maintained essentially constant amplitude up to temperatures where decomposition started. At this point the peak amplitude began to decline, and was matched by a concurrent growth in some other peak due to a pyrolysis product. Thus the degree of decomposition could be determined at several temperatures. The process was usually followed to essentially 100% decomposition.

The rate constant for the decomposition at any temperature is given by^{5a}

$$k_{\text{uni}} = k_{\text{ea}} f / (1 - f)$$

where k_{ea} is the rate of escape from the reactor (calculable from the dimensions of the reactor and the kinetic theory of gases) and f is the fraction of unimolecular reaction.

The rate constants thus obtained are not the first-order, high-pressure constants usually dealt with, but represent "falloff" rates due to the low pressures within the reactor. (See references 5a and 5h for detailed discussion of this topic.) The treatment of these data is described in the Results section.

Product Data--Our version of the VLPP reactor has the added capability of product isolation. A valved port in the manifold into which the reactor products pass, and in which the mass spectrometer head resides, leads to a liquid nitrogen cooled trap, and thus affords the opportunity of tapping the exit stream. The product isolation work was done after the kinetic runs were made, and the temperature ranges of interest were thus known. In agreement with the mass spectral data, the product distribution was reasonably constant throughout the temperature ranges for decomposition.

Products were collected for 30-60 min and then transferred under vacuum to sample vials. The samples were immediately diluted with pentane, and a gentle flow of nitrogen was passed over the samples to remove most of the nitric oxides present in the samples. The solutions were then analyzed by g.l.c. on a 20% carbowax 20 M column, programmed from 60 to 150°.

The products were identified through comparison in most cases with known samples of the compounds. The comparisons were made in terms of g.l.c. retention times, NMR, and mass spectra. Proof of the fact that the observed reactions were truly unimolecular and not wall catalyzed was provided by an experiment with 1,1-DNP in which product distribution was essentially unchanged for the three reactor exit apertures, corresponding to a change in wall collisions by a factor of over 100.

Results

Kinetic Data--An example of the treatment of the data obtained from our reactor is shown in Figure 1 for a series of calibration experiments with 2-nitropropane (2-NP). The details of this treatment are presented in reference 5h. Briefly, what has been done is that the established high-pressure rate constant for the unimolecular decomposition of 2-NP has been reduced to the falloff conditions in the reactor through the use of the Rice-Ramsperger-Kassel (RRK) theory of unimolecular reactions.⁷ Thus the solid curve in the figure represents the known first-order rate constant for the decomposition of 2-NP under the pressure and temperature conditions in the reactor. The experimental points fall close to the line, and this fit confirms the validity of our method.⁸

In Figure 2 are presented the VLPP data for the four dinitroalkanes. There is a fair amount of scatter in the points, much more than for 2-NP, and we have no explanation for this behavior. However, the data clearly fall into two families of points. Those points for the three gem-dinitro compounds reasonably well fall within the curves for k_1 and k_2 . In turn, k_1 and k_2 represent typical fall-off rate constants for the decomposition of gem-di- and trinitroalkanes from Table I with Arrhenius A-factors of 10^{17} sec^{-1} , and spanning activation energies from 46 and 48 kcal/mole.

The case for 1,2-DNP is different. If we ignore any possible next-nearest-neighbor effects, then 2-NP and 1,2-DNP should have the same Arrhenius parameters for cyclic HONO elimination. That is, at least to a first approximation,

$$k_{1\text{-NP}} = k_{1,2\text{-DNP}} = 10^{11.3-40/\theta} \text{ sec}^{-1}$$

The solid curve in Figure 2 is thus $k_{1,2\text{-DNP}}$ reduced to the falloff reactor conditions, and it is seen that the experimental data fit the curve reasonably well.⁹

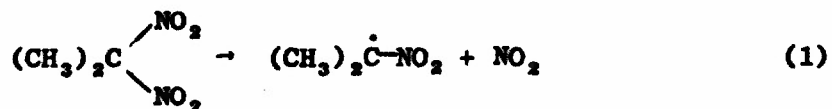
Product Data--The products from the VLPP studies of each of the compounds are shown in Table II.

Discussion

The nongeminate 1,2-DNP decomposed more slowly than did the other isomers, and yielded only nitropropenes. Both the product data and the kinetic parameters for the decomposition are in line with simple cyclic elimination of HONO for this compound.

Our kinetic data for the gem compounds on the other hand are consistent with the results of others in Table I. In view of the fact that our data result from experiments run at very low pressures, and thus under conditions where the rates of radical chain reactions should be vanishingly small, the suggestion that simple C-N scission is the major mode of decomposition of these compounds is confirmed.

The product data for the gem-dinitropropanes are consistent with C-N scission. The fact that carbonyl compounds are major decomposition products can be explained through a reaction sequence invoking a novel intramolecular oxygen transfer from N to C. Using 2,2-DNP as an example, the first step is C-N scission:



followed by migration of oxygen from nitrogen to carbon

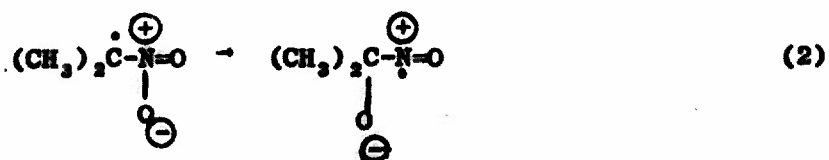


Table II
VLPP PRODUCTS FROM DINITROPROPANES^a

Compound	Products ^b	Relative Yield (%) ($\pm 5\%$) ^c
1,2-DNP	Acetone	55
	2-Nitropropene	45
1,1-DNP	Propionaldehyde	20
	<u>trans-1-Nitropropene</u>	5
	Unknown ^d	50
	Unidentified Products	25
1,1,1-FDNP	Propionyl Fluoride	only product isolated ^e
1,2-DNP	<u>trans-1-Nitropropene</u>	75
	2-Nitropropene	25

^a Flow through reactor 10^{15} - 10^{16} molecules/sec.

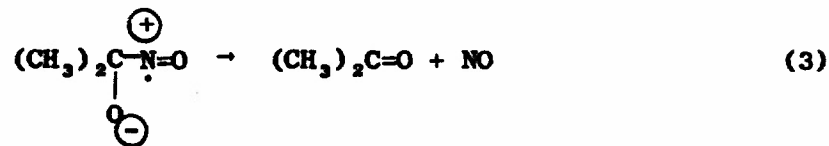
^b The product distributions were reasonably constant over the range of decomposition studied.

^c The mass balances for 1,1-DNP, 2,2-DNP, and 1,2-DNP were estimated to be 90% (see note e).

^d The unknown was unstable; its behavior and vpc retention time strongly suggest it to be nitroethylene.

^e The mass balance in this case was about 10%. The poor result probably is due to the high volatility of propionyl fluoride, resulting in a low trapping efficiency in these experiments.

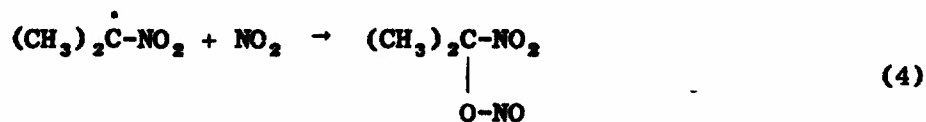
and subsequent loss of NO to form the carbonyl compound



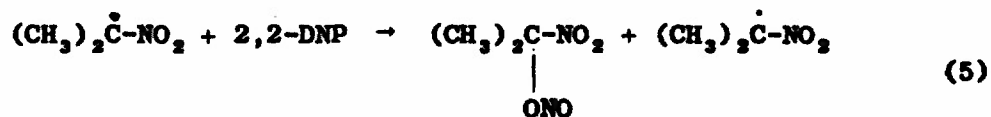
The net reaction is then



Flournoy^{3b} has reported the same stoichiometry from the pyrolysis of 2,2-DNP at pressures in the range of tens to hundreds of torr. He has suggested a radical chain process which includes the formation of an intermediate nitro-nitrite to explain the formation of a C-O bond.



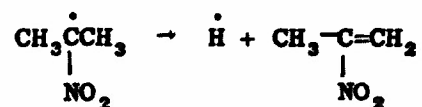
or



While reaction (5) is without precedent, (4) is likely under the relatively high-pressure conditions and could account for the results. In our work, however, the low pressures preclude such recombination, and thus reaction (2) is operative.¹⁰

The migration of O to C in these nitro radicals is reminiscent of F-migration we have observed in the case of the 2-difluoramino propyl radical.¹¹ However, while the rearrangement is about 40 kcal/mole exothermic in the fluorine case, it is roughly thermoneutral in the oxygen case.

The sequence 1-3 can therefore explain the formation of carbonyl-containing products in the case of all three gem-dinitroalkanes. The formation of nitroolefins, on the other hand, requires some parallel mechanistic route for the initially formed radical, most likely β -scission:



In summary, nongeminate dinitroalkanes, such as 1,2-dinitropropane, undergo simple cyclic HONO elimination, similar to their mononitro counterparts. The C-N bond weakening effect of α -nitro substitution in gem-dinitropropanes, on the other hand, lowers the C-N bond strength from a value of roughly 55-60 kcal/mole for simple mononitroalkanes, to values in the area of 47 kcal/mole. This lower value, plus the fact that the Arrhenius A-factor for the scission reaction is several orders of magnitude greater than that for cyclic HONO elimination, brings the rate of scission to a point where it is faster than elimination.

Acknowledgment

The work described was supported by the Office of Naval Research on Contract No. N00014-70-C-0190.

References

1. Nitromethane is the obvious, trivial exception.
2. For the collection of references in this area see: S. W. Benson and H. E. O'Neal, Kinetic Data on Gas-Phase Unimolecular Reactions, U.S. Department of Commerce, NSRDS-NBS 21.
3. (a) J. Sullivan and A. Axworthy, J. Phys. Chem., 70, 3366 (1966);
(b) J. Flournoy, J. Chem Phys., 36, 1107 (1962);
(c) G. M. Nazin, G. B. Manelis, and F. I. Dubovitskii, Bull. Acad. Sci. USSR, Div. of Chem. Sci., 374 (1968);
(d) Ibid., 2491;
(e) Ibid., 2494;
(f) Ibid., 2650.
4. Nazin et al, ^{3c-f} state that added gases, such as NO and NO₂, had no effect on the rate, and that the rate was moreover independent of the initial pressure. However, in one of the studies they cite, ^{3b} 2,2-dinitropropane decomposed apparently with significant radical chain contribution.
5. (a) S. W. Benson and G. N. Spokes, J. Amer. Chem. Soc., 89, 2525 (1967);
(b) G. N. Spokes and S. W. Benson, J. Amer. Chem. Soc., 89, 6030 (1967);
(c) S. W. Benson and G. N. Spokes, 11th Symposium (International) on Combustion, pp. 95-103 (1967);
(d) S. W. Benson and G. N. Spokes, J. Phys. Chem., 72, 1182 (1968);
(e) D. M. Golden, N. A. Gac, and S. W. Benson, J. Amer. Chem. Soc., 91, 2136 (1969);
(f) D. M. Golden, N. A. Gac, and S. W. Benson, J. Amer. Chem. Soc., 91, 3091 (1969);
(g) G. N. Spokes and S. W. Benson, in Recent Developments in Mass Spectroscopy, K. Ogata and T. Hayakawa, eds. (University Park Press, Maryland, 1970), p. 1146;
(h) K. D. King, D. M. Golden, G. N. Spokes, and S. W. Benson, Int. J. Chem. Kinetics, 3, 411 (1971);
(i) D. M. Golden, R. K. Solly, N. A. Gac, and S. W. Benson, J. Amer. Chem. Soc., 94, 363 (1972).

6. 1,1-DNP and 2,2-DNP, R. B. Kaplan and H. Schecter, J. Amer. Chem. Soc., 83, 3535 (1961); 1,2-DNP, N. Levy and C. Scaiti, J. Chem. Soc., 1103 (1946); 1,1,1-FDNP, V. Grakauskas and K. Baum, J. Org. Chem., 33, 3080 (1968).
7. G. Emanuel, Int. J. Chem. Kinetics, 4, 591 (1972). Tabulated values of the Kassel Integral are presented for convenient use in this and other applications.
8. Not shown are the results of a VLPP study in our reactor of i-propyl iodide in which the data are essentially indistinguishable from those of Benson et al.^{5h}
9. Under limiting high-pressure conditions, and at a given temperature, 2-NP and 1,2-DNP would be expected to decompose at the same rate. However, in the kinetic falloff region, at a given low pressure, since the dinitro molecule has a greater number of effective oscillators, its observed rate of decomposition would be expected to be greater than that for the simple nitroalkane. A careful comparison of the data in Figures 1 and 2 shows this to be the case.
10. Flournoy's reported rate constant in Table I,

$$\log k (2,2\text{-DNP}) = 18.5 - 51/\theta \quad (\text{k/sec}^{-1})$$

appears to have high A and E_a values compared to other values in Table I for other gem-dinitro compounds. At 190°C, the middle of the temperature range covered by Flournoy, this expression gives a rate of $10^{-5.3} \text{ sec}^{-1}$. In turn, this rate corresponds at that temperature to a second rate constant more in agreement with the parameters in Table I for gem-dinitroalkanes

$$\log k' (2,2\text{-DNP}) = 17.0 - 48/\theta \quad (\text{k/sec}^{-1})$$

Thus, Flournoy's results are consistent with the others.

11. D. S. Ross, T. Mill, and M. E. Hill, J. Amer. Chem. Soc., 94, 8776 (1972).

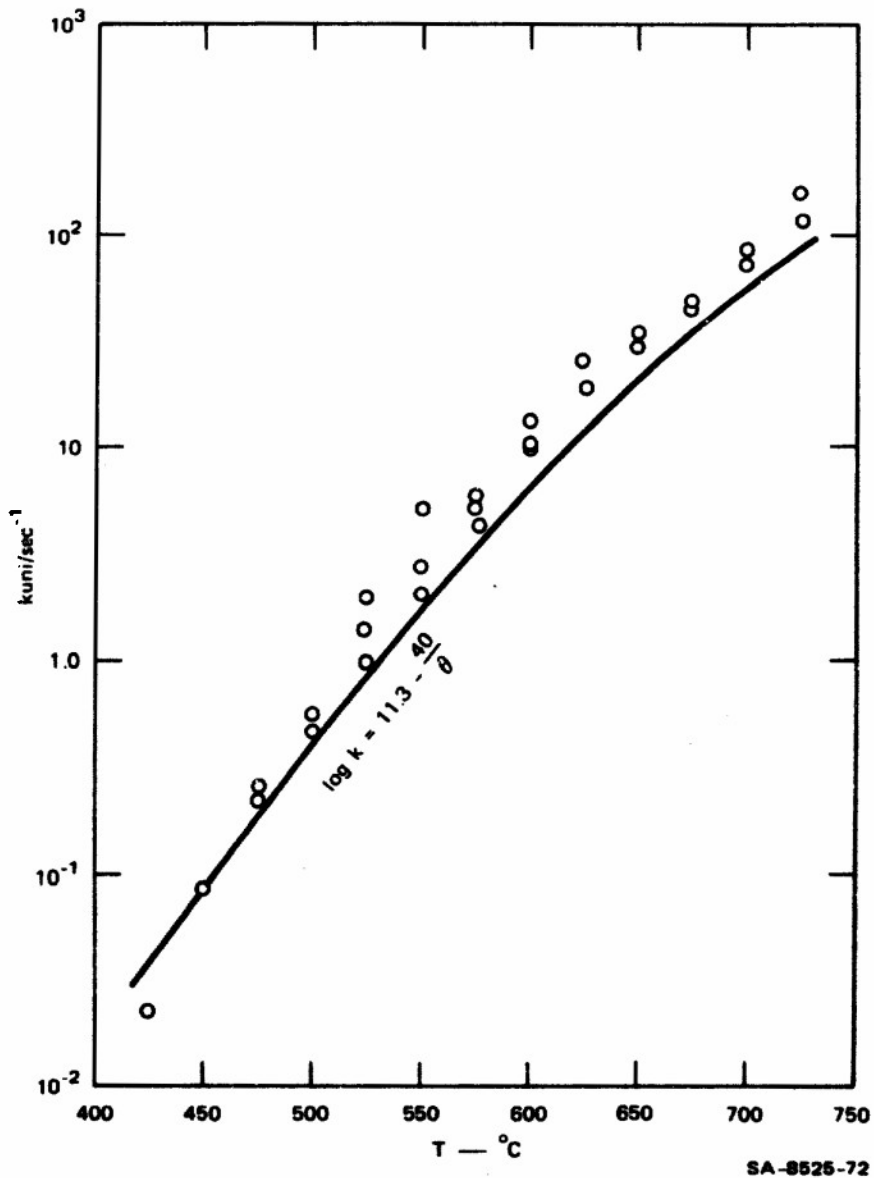


FIGURE 1 RATE CONSTANT VERSUS TEMPERATURE PLOT FOR TWO-NITROPROPANE

The solid curve corresponds to the known first-order rate constant for its unimolecular decomposition reduced down to the pressure and temperature conditions in the reactor. The circles are experimental points.

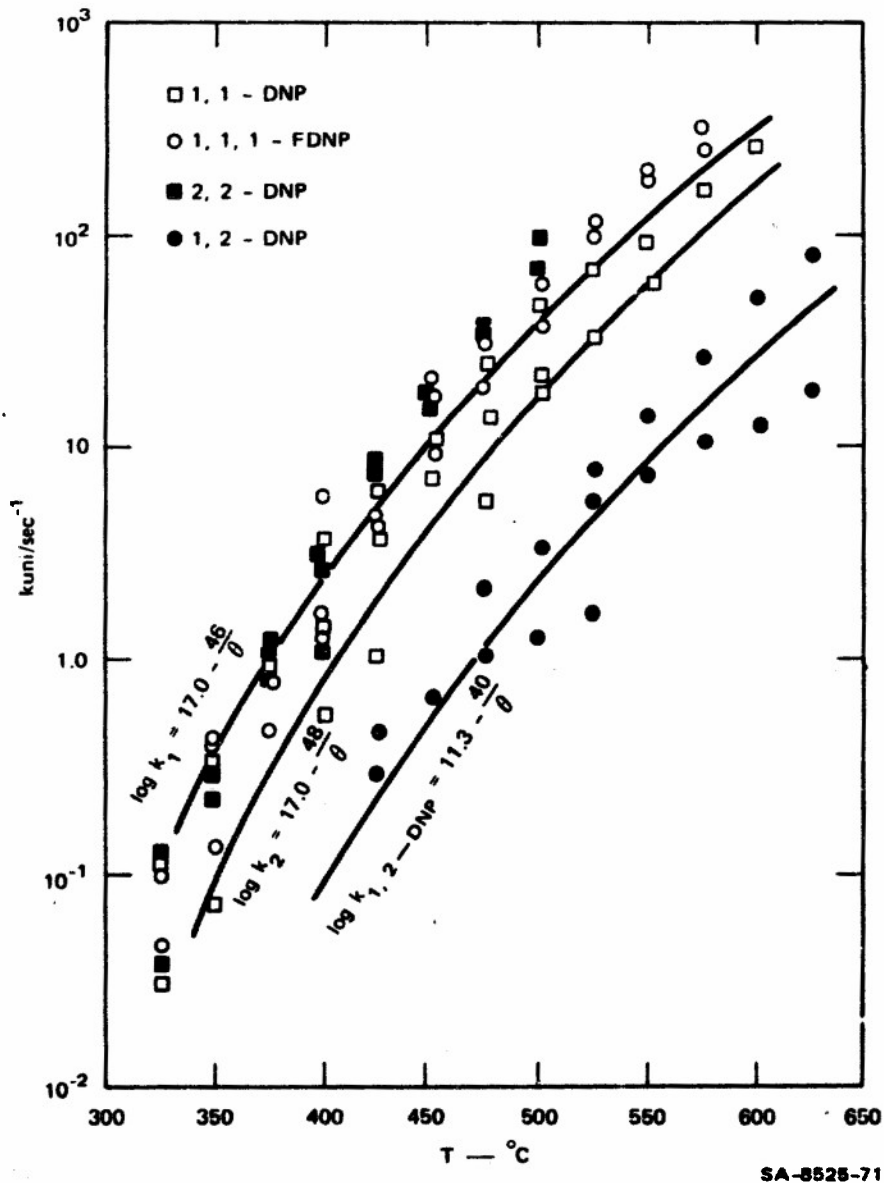


FIGURE 2 RATE VERSUS TEMPERATURE PLOT FOR FOUR DINITROPROPANES

REPORT DOCUMENTATION PAGE		READ INSTRUCTIONS BEFORE COMPLETING FORM	
1. REPORT NUMBER 8525 Final	2. GOVT ACCESSION NO.	3. RECIPIENT'S CATALOG NUMBER	
4. TITLE (and Subtitle) SENSITIVITY FUNDAMENTALS		5. TYPE OF REPORT & PERIOD COVERED Final Technical Progress Report, July ³¹ Dec 1975	
6. AUTHOR(s) T. Mill, D. S. Ross, N. A. Kirshen, C. M. Tarver, R. Shaw, and M. Cowperthwaite		6. PERFORMING ORG. REPORT NUMBER 8525-Final 75-2	
9. PERFORMING ORGANIZATION NAME AND ADDRESS Stanford Research Institute 333 Ravenswood Avenue Menlo Park, California		8. CONTRACT OR GRANT NUMBER(s) N00014-70-C-0190	
11. CONTROLLING OFFICE NAME AND ADDRESS Office of Naval Research Department of the Navy Arlington, Virginia		10. PROGRAM ELEMENT, PROJECT, TASK AREA & WORK UNIT NUMBERS 122402 85p.	
14. MONITORING AGENCY NAME & ADDRESS (if diff. from Controlling Office) NR-092-537 SRI-PYU-8525		12. REPORT DATE Mar. 19, 1976	13. NO. OF PAGES
16. DISTRIBUTION STATEMENT (of this report) Reproduction in whole or in part is permitted for any purposes of the United States Government.		15. SECURITY CLASS. (of this report) UNCLASSIFIED	
17. DISTRIBUTION STATEMENT (of the abstract entered in Block 20, if different from report)		15a. DECLASSIFICATION/DOWNGRADING SCHEDULE	
18. SUPPLEMENTARY NOTES NONE			
19. KEY WORDS (Continue on reverse side if necessary and identify by block number) sensitivity fundamentals low pressure pyrolysis detonation phenomena decomposition kinetics high pressure decomposition Dinitropropene (DNP) thermal explosion times activation energies activation volume failure diameter			
20. ABSTRACT (Continue on reverse side if necessary and identify by block number) Thermal decomposition of liquid 1,1-DNP at 1 and 1000 atm and 135-155 C gives over 90% propionic acid at conversions of 10-30%. The reaction is accelerated by pressure and by added water. 2,2-DNP decomposed slowly at 165 C to give only acetone, NO and NO ₂ . At 190 C 2,2-DNP had a half-life of 15 hours and gave acetone, acetic acid, CO ₂ , CO, and N ₂ O. Reactions of isobutane and neopentane with NO ₂ -N ₂ O ₄ indicated that HNO ₃ is an intermediate oxidizer in these reactions.			

19. KEY WORDS (Continued)

1,1-dinitropropane
2,2-dinitropropane
1,2-dinitropropane
1,1,1-fluorodinitropropane
1,1-dinitroethane
1- and 2-nitroalkanes
nitromethane
Dremin Trofimov model

20 ABSTRACT (Continued)

→ The gas-phase decompositions of four dinitropropanes have been studied, using low-pressure pyrolysis. 1,2-Dinitropropane undergoes cyclic elimination of HONO , to give 1- and 2-nitropropene; the rate constant for the process is $\log k (\text{sec}^{-1}) = 11.3 - 40/\theta$. The three gem-dinitroalkanes, 1,1- and 2,2-dinitropropane and 1-fluoro-1,1-dinitropropane undergo C-N scission with the same rate constant, $\log k (\text{sec}^{-1}) = 17.0 - (47 \pm 1)/\theta$. Products include propionaldehyde, and acetone and propionyl fluoride.

→ Detonation failure diameters of nitromethane, 1,1-dinitroethane, 1,1-dinitropropane, and 2,2-dinitropropane were measured for the cases of heavy confinement in thick-walled lead cylinders and Dremin's weak shell confinement. Shock-induced reaction times and failure wave velocities in decaying detonation waves were also measured and used in the Dremin-Trofimov model to calculate failure diameters of the unconfined liquids. ↗